

-

CLS-DOS-NT-04-255

Version : 1rev0 of the 10 December 2004

Nomenclature : -

**Final Report on activities performed in 2002-2004 on the
ERS2/MWR survey**

		<u>COMPANY</u>	<u>DATE</u>	<u>INITIALS</u>
WRITTEN BY	M. Dedieu L. Eymard E. Obligis N. Tran	CETP LODYC CLS CLS		
CHECKED BY	M. Destouesse	CLS		
APPROVED BY	OZ. Zanife	CLS		
APPLICATION AUTHORISED BY	P. Féménias	ESA		

CLS -	Final Report on activities performed in 2002-2004 on the ERS2/MWR survey	Page : 1 Date : 2004-12-10
Source ref : CLS-DOS-NT-04-255	Nomenclature : -	Issue : 1 rev. 0

APPLICABLE DOCUMENTS / REFERENCE DOCUMENTS

Reference documents :

- Cyclic reports (e-mail)
- L. Eymard and SA Boukabara, , Calibration – validation of the ERS-2 microwave radiometer. Final report of the contract 11031/94/NL/CN, 1997
- L. Eymard and S.A. Boukabara, Report on the MWR anomaly, September, 1996
- L.Eymard and E. Obligis, preliminary report on long term stability of ERS2/MWR over continental areas, December, 1999.
- L. Eymard, E. Obligis, and N. Tran, ERS-2 MWR drift evaluation and correction, Report CLS/DOS/NT/03.688, February 2003.
- F. Mertz, N. Tran, S. Labroue, J. Dorandeu, V. Marrieu, J. Savaresse, ERS2 OPR data quality assessment (Long-term monitoring and particular investigations)- Annual report 2004 of task 2 of IFREMER Contract No 04/2.210.714.
- E. Obligis, Analysis of the side lobe contribution in case of the ENVISAT/MWR. Report no CLS/DOS/NT/01.37
- E. Obligis, restitution des paramètres géophysiques : évaluation des performances globales de la méthode ; nouvelle méthode d'étalonnage/validation. Final report of the contract CNES O1425/5200-6000, January 2000.
- E. Obligis and S. Labroue, analysis of Neural network retrieval algorithms for the ENVISAT/MWR . Report CLS/DOS/NT/01.37, September, 2001.
- Ruf, C.S., 2000: Detection of calibration drifts in spaceborne microwave radiometers using a vicarious cold reference. IEEE Trans. Geosci. Remote Sens., 38(1), 44-52.
- M. Dedieu, L. Eymard, C. Marimont, E. Obligis, N. Tran, 2003 : Final Report on activities performed in 2002-2004 on the ERS2/MWR survey .

CLS -	Final Report on activities performed in 2002-2004 on the ERS2/MWR survey	Page : 2 Date : 2004-12-10
Source ref : CLS-DOS-NT-04-255	Nomenclature : -	Issue : 1 rev. 0

CONTENTS

1. INTRODUCTION	3
2. MISSION OVERVIEW	5
3. ROUTINE SURVEY OF THE MWR.....	6
3.1. SURVEY OF THE MAIN INSTRUMENTAL PARAMETERS	6
3.2. MAPS OF THE BRIGHTNESS TEMPERATURES OVER SOUTH POLE.....	9
3.3. MONITORING OF COLD OCEAN BRIGHTNESS TEMPERATURES	11
4. CALIBRATION.....	12
4.1. COMPARISON BETWEEN MEASUREMENTS AND SIMULATIONS	12
4.2. STABILITY ANALYSIS ON STABLE CONTINENTAL AREAS.....	13
5. VALIDATION	14
6. CORRECTION FOR THE 23.8 GHZ DRIFT.....	18
7. FINAL COMMENTS AND RECOMMENDATIONS	19
8. ANNEX 1	20
9. ANNEX 2	67

CLS -	Final Report on activities performed in 2002-2004 on the ERS2/MWR survey	Page : 3 Date : 2004-12-10
Source ref : CLS-DOS-NT-04-255	Nomenclature : -	Issue : 1 rev. 0

1. INTRODUCTION

The statement of work for the long term survey of the ERS2 microwave radiometer (MWR) by CETP and CLS included the following issues:

- continuous monitoring of the key instrumental parameters, to detect any anomaly ; detailed analysis of anomalies if observed ;
- long term analysis of the brightness temperatures over stable natural targets, to evaluate the instrument stability and quantify any drift.

Since the beginning of the contract in September 2002, the main activities have concerned:

- Extraction of data from the Kiruna station via the ESRIN server then automatically processed at CETP.
- Anomalies in the data (missing data, or telemetry format problems) have been identified and messages sent to ESRIN.
- At the end of every cycle, an assessment report is sent to ESRIN, with the plots of the main instrumental parameters, the maps of the brightness temperatures over the South Pole, the survey of the coldest ocean points.
- In parallel to these routine activities, calibration / validation evaluations have been performed, by comparing measured brightness temperatures with simulated ones from ECMWF fields, and by comparing the tropospheric correction (or water vapour) with radiosonde data over oceans. Evaluation of the neural ENVISAT algorithms has been performed on ERS2 data.
- An evaluation of the absolute calibration of the ERS2/MWR has been performed using hot and cold continental targets. It appears that the 23.8 GHz channel is perfectly well calibrated whereas the 36.5 GHz brightness temperatures appear too high for hot brightness temperatures.

<p style="text-align: center;">CLS</p> <p style="text-align: center;">-</p>	<p style="text-align: center;">Final Report on activities performed in 2002-2004 on the ERS2/MWR survey</p>	<p>Page : 4</p> <p>Date : 2004-12-10</p>
<p>Source ref : CLS-DOS-NT-04-255</p>	<p>Nomenclature : -</p>	<p>Issue : 1 rev. 0</p>

- Finally, a study of the long term stability of ERS2/MWR has been achieved, using data from four land cold and hot targets, and using the coldest ocean points. This study has been used to propose in February 2003 a correction for the 23.8 GHz drift.

The following report summarizes the work performed in the framework of the contract since September 2002. For each activity, we will give the status, main steps and results.

CLS -	Final Report on activities performed in 2002-2004 on the ERS2/MWR survey	Page : 5 Date : 2004-12-10
Source ref : CLS-DOS-NT-04-255	Nomenclature : -	Issue : 1 rev. 0

2. MISSION OVERVIEW

Since the launch of ERS2, two major events have been noticed:

1) The anomaly on the 23.8 GHz channel which occurred in June, 1996. This anomaly is probably due to the failure of an amplifier, leading to a decrease of the gain by a factor of about 10. Despite this problem, the sensitivity of the channel is still good enough, enabling to retrieve the tropospheric path correction with an accuracy similar to Topex/TMR one. To use the standard algorithms, a linear correction was established, using data from the first year as reference. This work is described in the final report of the in-flight calibration / validation (Eymard and Boukabara, 1997).

2) Due to a failure of the ERS-2 tape recorder on 22 June 2003, the recording capabilities are permanently unavailable. The ERS-2 tape recorders were used to record the ERS-2 Low Rate mission globally, after 8 years of continuous acquisition this service is now discontinued. The ERS-2 Low Rate mission goes on within the visibility of ESA ground stations over Europe, North Atlantic, the Arctic and western North America.

CLS -	Final Report on activities performed in 2002-2004 on the ERS2/MWR survey	Page : 6 Date : 2004-12-10
Source ref : CLS-DOS-NT-04-255	Nomenclature : -	Issue : 1 rev. 0

3. ROUTINE SURVEY OF THE MWR

The assessment report produced at the end of every 35-day cycle shows the behaviour of ERS2 Microwave Radiometer in terms of instrumental characteristics and quality of the brightness temperatures. It is performed on the MWR level 0 data product (EMWC). The decoding and the pre-processing are done with the MWR level 1B reference processing chain located at CETP. The data are from the Kiruna station (KS), the Maspalomas Station (MS), the Prince Albert Station (PS) and the Gatineau Station (GS).

The objectives of this document are:

- to provide an instrumental status;
- to check the stability of the instrument;
- to report any change at the instrumental level likely to impact quality of the brightness temperatures;
- to check the stability of the brightness temperatures.

3.1. SURVEY OF THE MAIN INSTRUMENTAL PARAMETERS

Figure 1 shows the gain since the anomaly in June, 1996, and a zoom on the last 10% data. The stability of the gain on the two channels is remarkable. Slight variations, which do not exceed a few %, can be observed with time. Even when the instrument was switched off/on, the gain has come back close to each nominal value. Note that the gain of the 36.5 GHz presents a continuous, but very weak increase with time, due probably to the evolution of the receiver. Figure 2 and 3 show respectively the variations of the hot and cold counts and of the residual temperature. Except, the noise which is higher for the 23.8 GHz channel due to the gain drop, the variations are very weak and the small drifts observed remain acceptable .

CLS -	Final Report on activities performed in 2002-2004 on the ERS2/MWR survey	Page : 7 Date : 2004-12-10
Source ref : CLS-DOS-NT-04-255	Nomenclature : -	Issue : 1 rev. 0

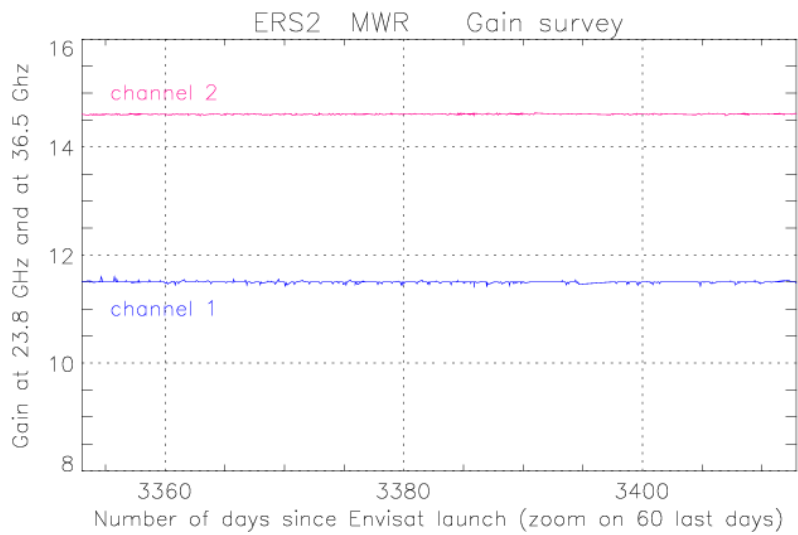
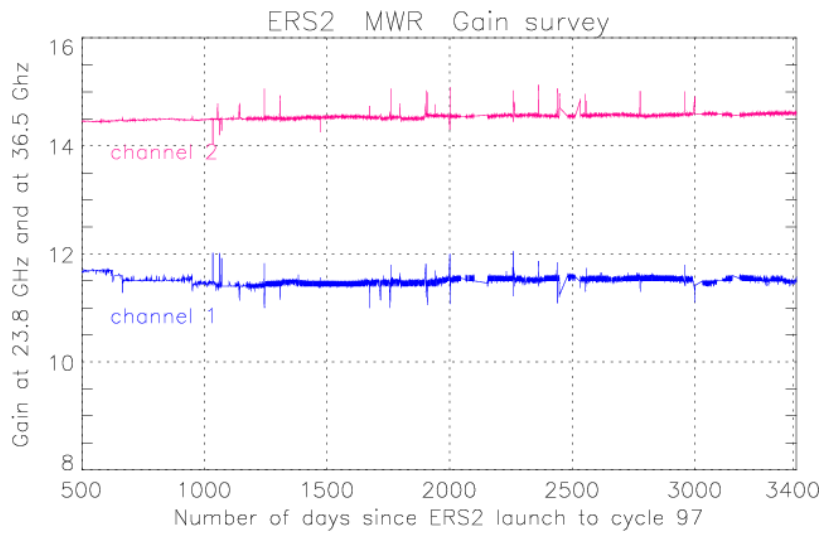


figure 1

<p style="text-align: center;">CLS</p> <p style="text-align: center;">-</p>	<p style="text-align: center;">Final Report on activities performed in 2002-2004 on the ERS2/MWR survey</p>	<p>Page : 8</p> <p>Date : 2004-12-10</p>
<p>Source ref : CLS-DOS-NT-04-255</p>	<p>Nomenclature : -</p>	<p>Issue : 1 rev. 0</p>

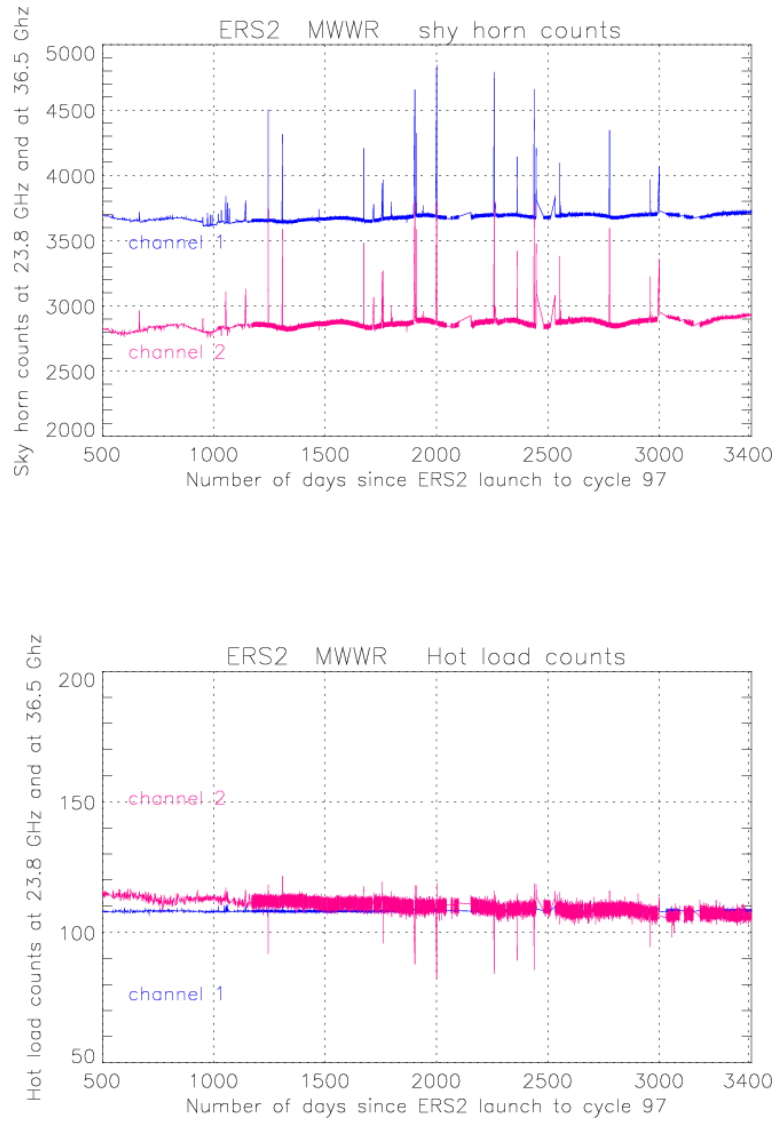


Figure 2

CLS -	Final Report on activities performed in 2002-2004 on the ERS2/MWR survey	Page : 9 Date : 2004-12-10
Source ref : CLS-DOS-NT-04-255	Nomenclature : -	Issue : 1 rev. 0

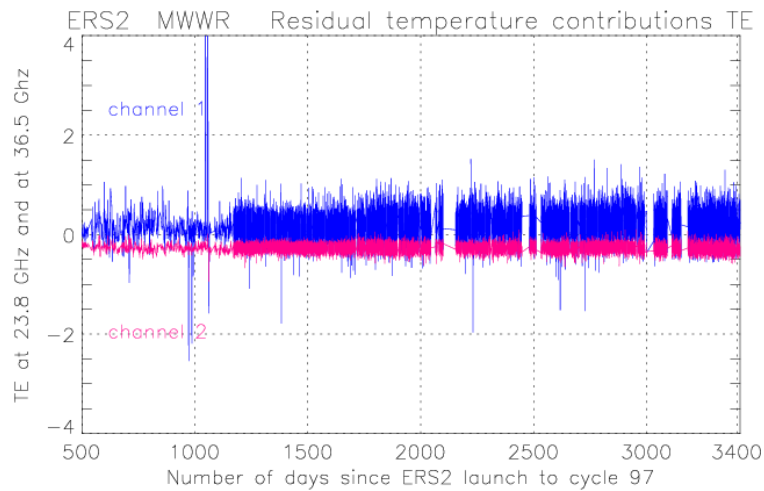


Figure 3

3.2. MAPS OF THE BRIGHTNESS TEMPERATURES OVER SOUTH POLE

Over poles, the space and time coverages are sufficient to draw maps of the brightness temperatures. Since the atmospheric variability is weak due to the very low water vapour content, the brightness temperatures are mainly representative of surface emissivity and temperature variations, which slowly vary within the course of the year. Consequently, the South Pole can be used as a stable target to monitor the brightness temperature variations with time. Figures 4 (top) and (bottom) show respectively the 23.8 and 36.5 GHz brightness temperatures measured by the radiometer over the South Pole (latitudes higher than 65°S) for the last cycle (85). The ice cap appears colder than the sea ice and the free water at the two frequencies.

<p>CLS -</p>	<p>Final Report on activities performed in 2002-2004 on the ERS2/MWR survey</p>	<p>Page : 10 Date : 2004-12-10</p>
<p>Source ref : CLS-DOS-NT-04-255</p>	<p>Nomenclature : -</p>	<p>Issue : 1 rev. 0</p>

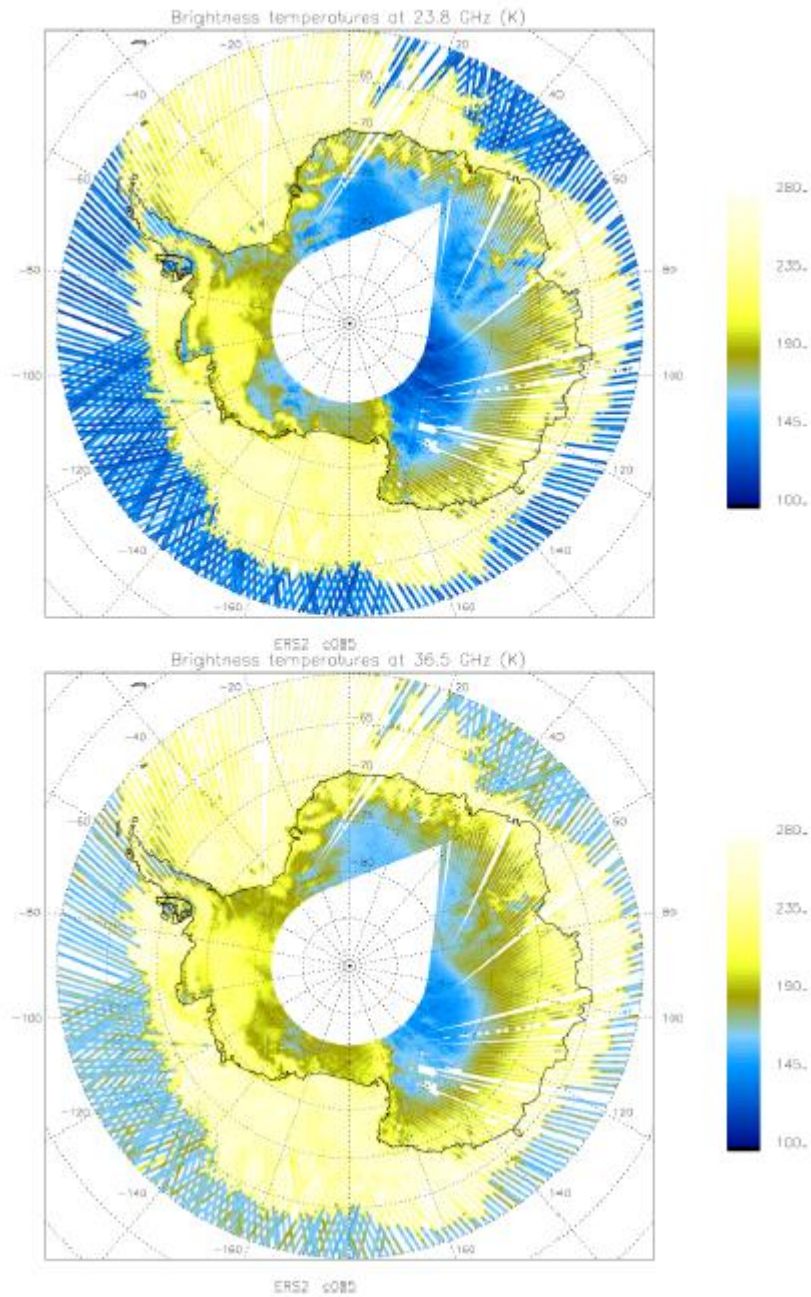


Figure 4

CLS -	Final Report on activities performed in 2002-2004 on the ERS2/MWR survey	Page : 11 Date : 2004-12-10
Source ref : CLS-DOS-NT-04-255	Nomenclature : -	Issue : 1 rev. 0

3.3. MONITORING OF COLD OCEAN BRIGHTNESS TEMPERATURES

To assess the long term stability of the radiometer, monitoring the coldest measurements over ocean was performed. This method, derived from Chris Ruf's one for TMR (Ruf, 2000), was found to be the most efficient, to point out possible slight trends. The method consists of first filtering out data with value higher than a given threshold, then filtering out again the remaining data with values above the cycle average minus 1.5 times the standard deviation. The resulting time series is plotted in figure 5. The perfect stability of 36.5 GHz channel is confirmed, and a trend is clearly depicted on the first channel. The study and correction of this drift is the purpose of chapter 6.

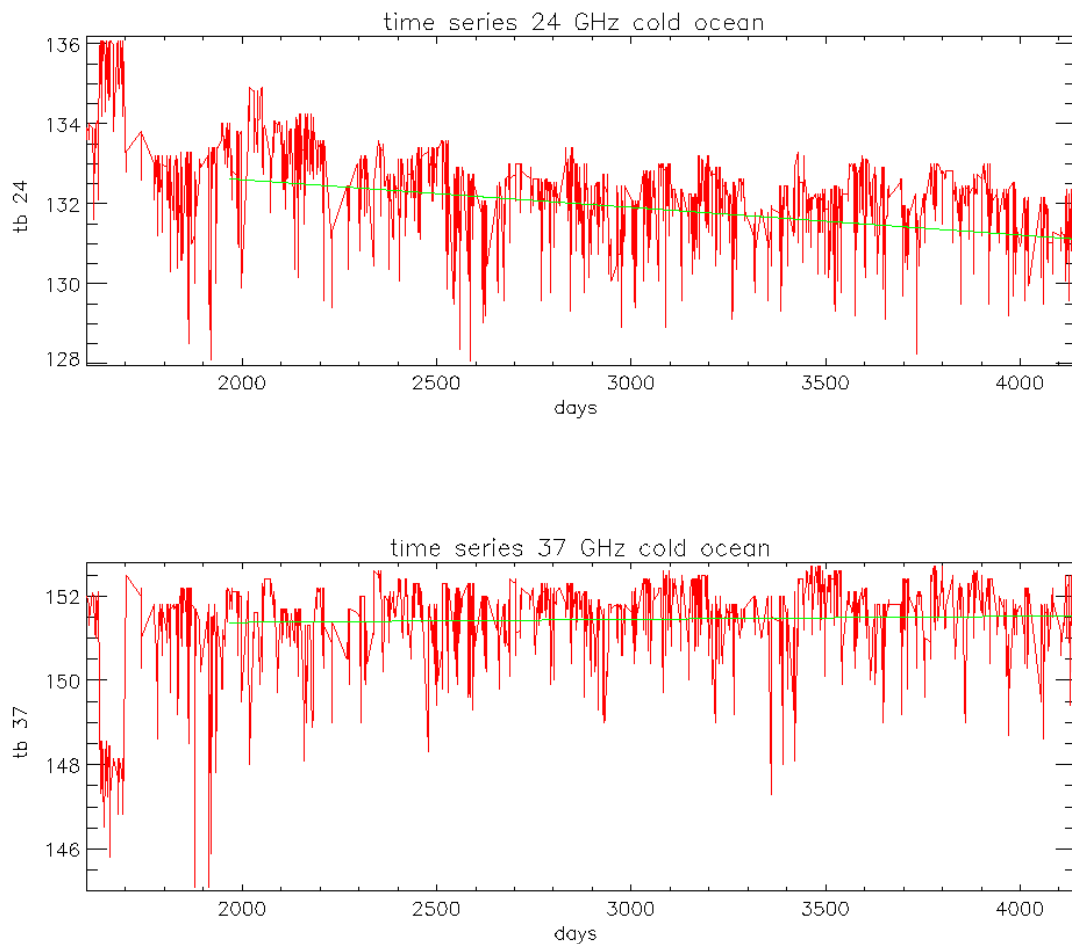


figure 5

CLS -	Final Report on activities performed in 2002-2004 on the ERS2/MWR survey	Page : 12 Date : 2004-12-10
Source ref : CLS-DOS-NT-04-255	Nomenclature : -	Issue : 1 rev. 0

4. CALIBRATION

4.1. COMPARISON BETWEEN MEASUREMENTS AND SIMULATIONS

The MWR measurements (brightness temperatures and backscattering coefficient) have been compared with simulations (figure 6). The methodology is the following:

- selection of several ECMWF analyses (output fields containing temperature and humidity profiles, cloud amount, surface wind and temperature);
- co-location of satellite and model points, by averaging satellite data falling in given intervals (± 1 hours, $\pm 1^\circ$) within a model grid mesh;
- simulation of the instrument brightness temperature and comparison with the measurement in clear conditions (filtering out cloudy pixel using model cloud information and a liquid water algorithm and threshold on the radiometer data).

For the last years, we used the UCL model, after improvement by Boukabara (1997). Its advantage is a more sophisticated electromagnetic surface model, allowing us to simulate both the MWR and the altimeter measurements.

The results of these comparisons show a good correlation between measurements and simulations. Biases are around 3-4K and the standard deviation around 5K. Note the very good agreement between measurements and simulations at 23.8 GHz (primary channel), that insures the good behaviour of the retrieval algorithm.

CLS -	Final Report on activities performed in 2002-2004 on the ERS2/MWR survey	Page : 13 Date : 2004-12-10
Source ref : CLS-DOS-NT-04-255	Nomenclature : -	Issue : 1 rev. 0

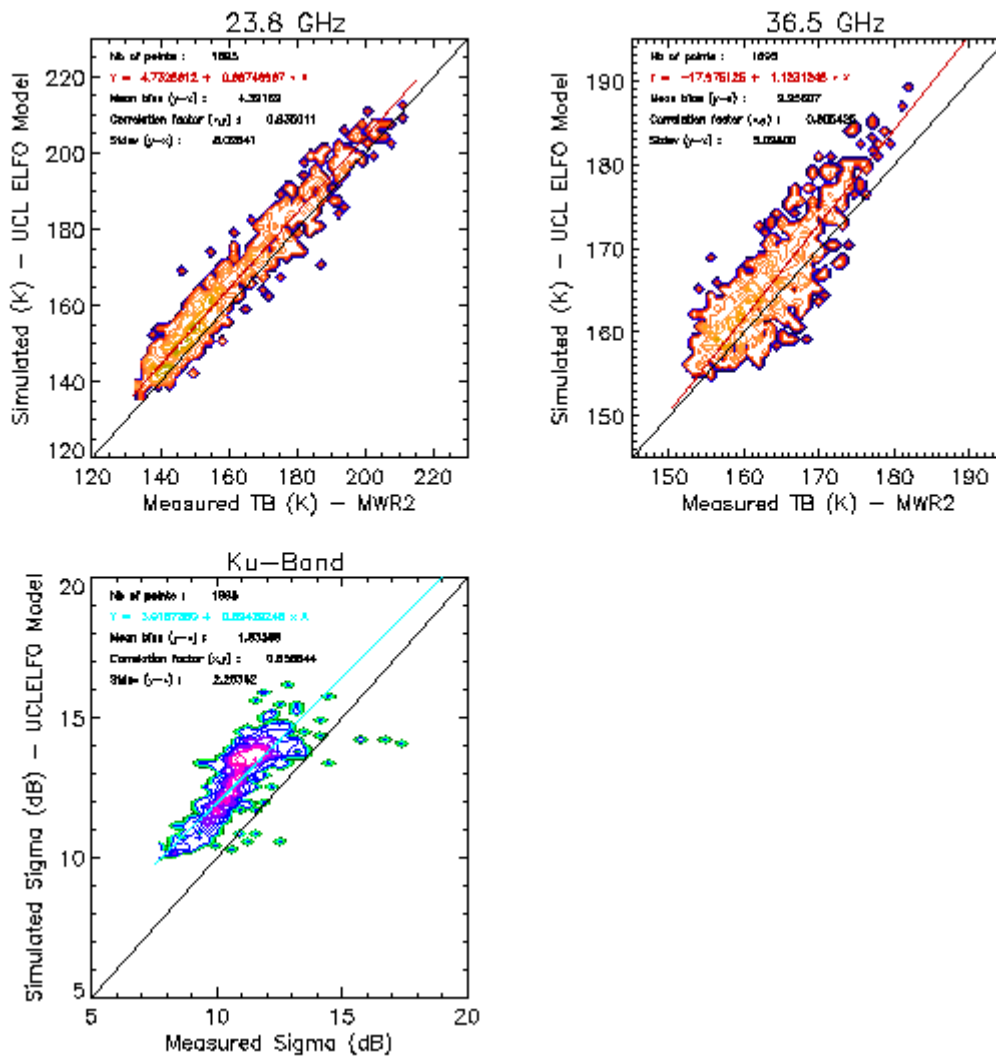


Figure 6

4.2. STABILITY ANALYSIS ON STABLE CONTINENTAL AREAS

This study is part of a paper submitted in 2004 in IEEE Transactions on Geoscience and Remote Sensing. The revised version of the paper with all results is provided in annex 1 of this document.

CLS -	Final Report on activities performed in 2002-2004 on the ERS2/MWR survey	Page : 14 Date : 2004-12-10
Source ref : CLS-DOS-NT-04-255	Nomenclature : -	Issue : 1 rev. 0

5. VALIDATION

Validation of an instrument as the MWR is difficult because of its field of view. The method we have applied since ERS-1 is to compare the tropospheric path corrections from the radiometer with calculated ones from measured vertical profiles over oceans. Then collocation within a given interval (± 1 hour in time and 100 km in distance) is made before drawing the scatter plot. The Figure 7 shows the last results, obtained for a 8-year period. Here the standard ERS-2 algorithm is directly applied to measurements (those of the 23.8 GHz channel are corrected for the anomaly). The result is satisfactory: despite the anomaly, the retrieved tropospheric path corrections are in good agreement with the measured ones. The mean bias is of 6 mm and the rms error of 1.8 cm (not corrected from the bias). But this value does not give an estimation of the absolute rms error of the wet tropospheric correction since it takes into account, error on the radiosondes measurement, error of colocalisation, and atmospheric variability within the time and distance frame.

CLS -	Final Report on activities performed in 2002-2004 on the ERS2/MWR survey	Page : 15 Date : 2004-12-10
Source ref : CLS-DOS-NT-04-255	Nomenclature : -	Issue : 1 rev. 0

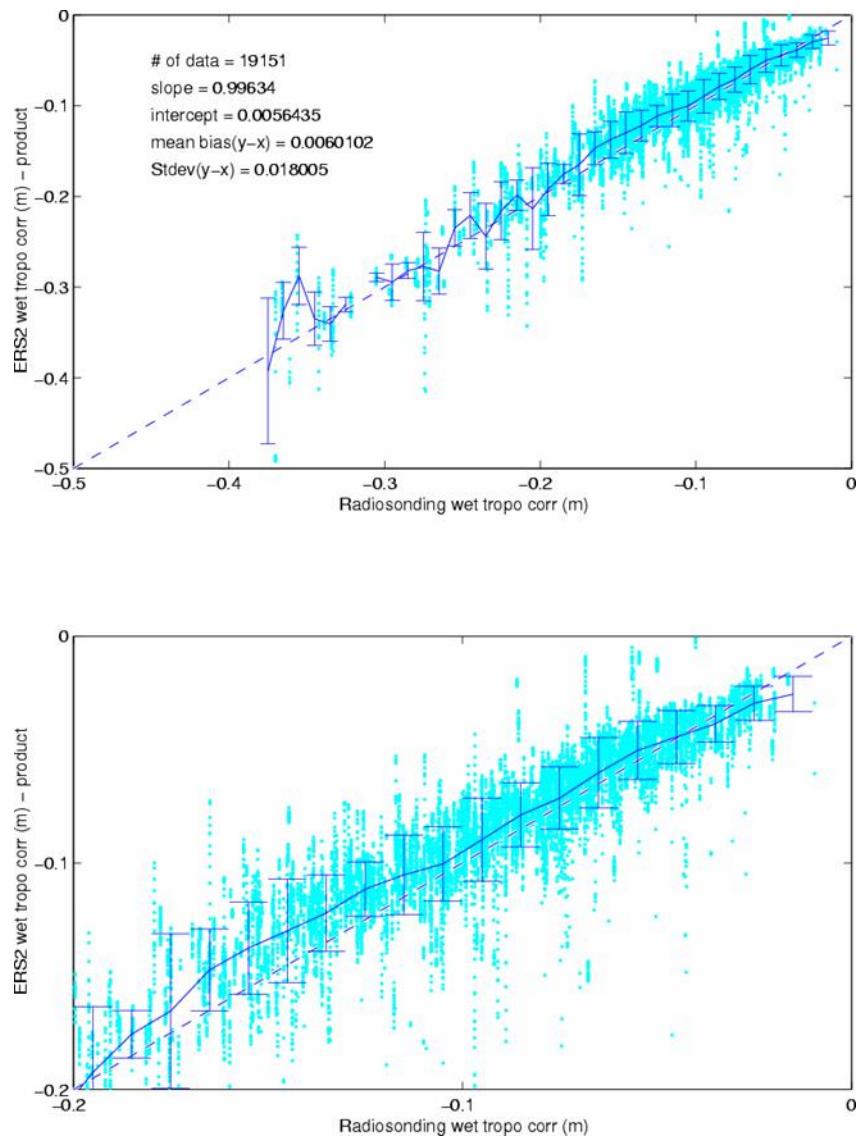


Figure 7

Our recent progresses on retrieval method (updated regression algorithm, and use of neural network) suggest that an update of the ERS2 processing could be made, to bring the ERS2 retrieved data in line to ENVISAT ones of higher accuracy. Furthermore the ERS-2 algorithm for the wet tropospheric correction was found to be biased in dry situations (very low water vapour content), and the algorithm developed for ENVISAT corrects well for this bias as showed in the following results. A technical note that explains how to apply the ENVISAT algorithm on ERS-2 data along with fortran and C routines are available to ERS2 users (Tran and Obligis, 2003) to implement them. This analysis did also serve to validate the ENVISAT

CLS -	Final Report on activities performed in 2002-2004 on the ERS2/MWR survey	Page : 16 Date : 2004-12-10
Source ref : CLS-DOS-NT-04-255	Nomenclature : -	Issue : 1 rev. 0

neural algorithm and products with radiosonde data to check the quality and reliability of the new retrieval. Because at the time of the study, we did not get enough collocations between radiosondes and ENVISAT wet tropospheric correction measurements. In order to provide a first assessment of the quality of ENVISAT wet tropospheric correction (neural algorithm) with radiosonde measurements, we computed the new ERS2 wet tropospheric correction and then use a previous compilation of ERS2/radiosondes.

Biases and correction have to be applied on ERS2 data as a pre-processing step to have algorithm inputs as similar as possible between the two instruments to allow optimum use of the algorithms and provide less biased retrieved products. The ERS2 TBs at 23.8 GHz were corrected for the drift as proposed in Obligis et al (2003) in all presented results. Table 1 provides the biases between ENVISAT and ERS2 TBs for both channels computed on ENVISAT cycle 010. These values have to be added to the respective ERS2 TB products.

Cycle 010	TB 23.8 GHz (K)	TB 36.5 GHz (K)	attenuation (dB)
ENV/ERS2	2.98	2.39	2.09 ers2 + 0.09

Table 1

A linear relationship for the Ku-band atmospheric attenuation correction between the two instruments is also provided because ENVISAT sigma-naught has been calibrated on ERS2 corrected values and the radiometric algorithms were evaluated on uncorrected ones. In the formulation of ERS2 attenuation correction model only the absorption by cloud liquid water has been taken into account, while for ENVISAT a more complex model has been used. It takes also into account gaseous absorption by oxygen and water vapour. So this linear relationship provides a new attenuation correction term that has to be removed from the ERS2 corrected sigma-naught product. Plots on Figure 8 were obtained with the drift correction applied and the ENVISAT neural algorithm. The slopes and intercepts for the orthogonal distance regression line are provided. We get a better agreement with the radiosonde measurements when the drift correction and the ENVISAT algorithm are applied. The improvement due to both the drift correction and the neural algorithm is better pointed out by the bin averaging also computed. It is especially obvious for wet tropospheric corrections lower in absolute value than 0.1 m, where most of the data are.

CLS -	Final Report on activities performed in 2002-2004 on the ERS2/MWR survey	Page : 17 Date : 2004-12-10
Source ref : CLS-DOS-NT-04-255	Nomenclature : -	Issue : 1 rev. 0

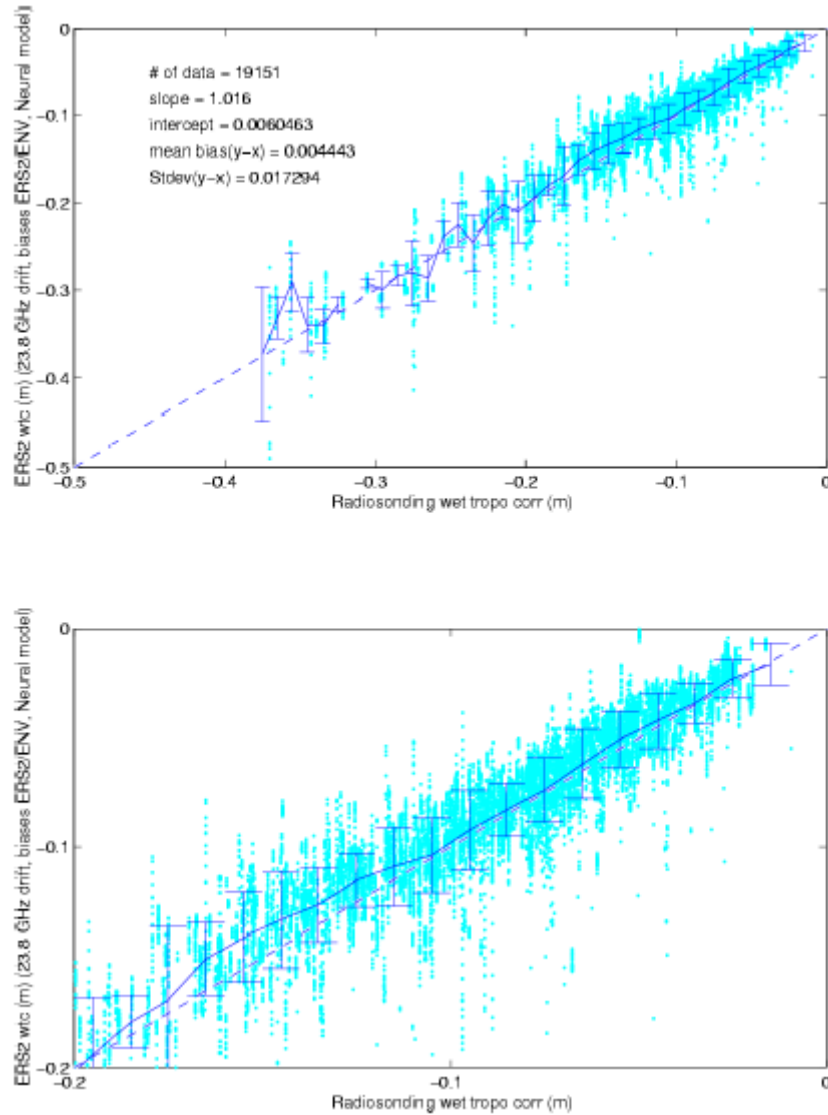


Figure 8

Finally, in the framework of the preparation of ENVISAT mission, a particular study has been conducted to take into account the contamination by the secondary lobes (a large effect was expected due to the big efficiency coefficient of the platform for the 23.8 GHz channel). In this context, we have checked, using particular tracks, that there is no significant signal due to a contamination by the secondary lobe on ERS2 brightness temperatures (Dedieu et al, 2003).

<p style="text-align: center;">CLS</p> <p style="text-align: center;">-</p>	<p style="text-align: center;">Final Report on activities performed in 2002-2004 on the ERS2/MWR survey</p>	<p>Page : 18</p> <p>Date : 2004-12-10</p>
<p>Source ref : CLS-DOS-NT-04-255</p>	<p>Nomenclature : -</p>	<p>Issue : 1 rev. 0</p>

6. CORRECTION FOR THE 23.8 GHZ DRIFT

Two corrections (gain drop + drift) are presently available at this time, Eymard et al (2003) and Scharroo et al (2004). So a comparison analysis was performed in the framework of 2004 activities of task 2 (ERS2 OPR data quality assessment) of IFREMER Contract No 04/2.210.714 (Mertz et al, 2004). The results are provided in annex 2 for information.

CLS -	Final Report on activities performed in 2002-2004 on the ERS2/MWR survey	Page : 19 Date : 2004-12-10
Source ref : CLS-DOS-NT-04-255	Nomenclature : -	Issue : 1 rev. 0

7. FINAL COMMENTS AND RECOMMENDATIONS

Since the beginning of the mission, the ERS2 radiometer is compliant with the initial specifications.

In 2003, we proposed a correction for the 23.8 GHz drift, based on the survey of the coldest ocean points. In 2004, Scharroo et al proposed a new correction and a recent evaluation of both corrections revealed that the second one was more accurate (use of a longer time series and nonlinear regression). We therefore recommend to the users to apply this latter. This drift correction ensures a better stability of the retrieved products, especially for estimation of the long term sea level change.

Algorithmic improvements performed for the ENVISAT mission, have been tested on ERS2 data and it appears that they improve the products. We therefore recommend to the users the use of these new neural algorithms.

The absolute calibration of the radiometer has been analysed in details using different methods (continental hot and cold targets, emissivity estimations over the Amazon forest) and the concluding remarks are that the 23.8 GHz channel of the radiometer is well calibrated, whereas, the hot brightness temperatures at 36.5 GHz are too high. These results should be kept in mind when performing a new calibration of the ENVISAT radiometer.

CLS -	Final Report on activities performed in 2002-2004 on the ERS2/MWR survey	Page : 20 Date : 2004-12-10
Source ref : CLS-DOS-NT-04-255	Nomenclature : -	Issue : 1 rev. 0

8. ANNEX 1

Long term stability of ERS2 and TOPEX microwave radiometer in-flight calibration

Laurence Eymard* (1), Estelle Obligis (2), Ngan Tran (2), Fatima Karbou (3),
Antoine Pilon (3) and Michel Dedieu (3)

(1) CNRS/IPSL/LODYC, 4 place Jussieu, Paris, France

(2) CLS, Ramonville St-Agne, France

(3) CNRS/IPSL/CETP, Vélizy, France

Abstract :

The microwave radiometers on altimeter missions are specified to provide the “wet” troposphere path delay with an uncertainty of 1 cm or lower, at the location of the altimeter footprint. The constraints on the calibration and stability of these instruments are therefore particularly stringent. The paper addresses the questions of long term stability and the absolute calibration of the NASA TOPEX and ESA ERS2 radiometers over the entire range of brightness temperatures. Selecting the coldest measurements over ocean from the two radiometers, the drift of the TOPEX 18 GHz radiometer channel is confirmed to be about 0.2 K/year over the seven first years of the mission, and the one of the ERS2 radiometer 23.8 GHz channel to be -0.2 K/year. The good stability of the other channels is evidenced (drift less than 0.04 K/year). The use of continental targets for analyzing the long term drift is evaluated: the natural inter-annual variability prevents one from directly monitoring the drift of each channel, but the relative variation between two channels of the same instrument is found consistent with the cold ocean analysis. Intercomparison of radiometer absolute calibrations is performed over the same continental area, leading to an anomalously high difference between channels 36.5 and 37 GHz of the ERS2 and TOPEX radiometers, respectively, over “hot” targets (Sahara desert and Amazon forest). To quantify and analyze this difference, other radiometer measurements are taken over the Amazon forest, from the Special Sensor Microwave Imager (SSM/I) and the Advanced Microwave Sounding Unit (AMSU). Biases are confirmed for both TOPEX and ERS2 radiometers by comparing brightness temperatures and retrieved surface emissivities: The TOPEX radiometer channels exhibit a negative bias with respect to SSMI and AMSU-A, whereas the ERS2 radiometer 36.5 GHz channel is positively biased, both by several Kelvin in brightness temperature. The

CLS -	Final Report on activities performed in 2002-2004 on the ERS2/MWR survey	Page : 21 Date : 2004-12-10
Source ref : CLS-DOS-NT-04-255	Nomenclature : -	Issue : 1 rev. 0

method presented here could be used for controlling the in-flight calibration of any radiometer, and correct for remaining calibration errors after launch.

Submitted to IEEE Transactions on Geoscience and Remote Sensing, 2004

* formerly at CNRS/IPSL/CETP, Vélizy.

1. Introduction

The microwave radiometers on board altimeter satellites are specified to provide the “wet” troposphere path delay with an uncertainty of 1 cm or lower, at the location of the altimeter footprint (any bias in the tropospheric correction directly impacts the sea level determination). They continuously measure the natural radiation from the atmosphere and surface at the vertical below the satellite. These instruments have two or three channels, including one in the water vapor absorption line centered at 22.235 GHz in order to properly retrieve the path delay (Bernard et al, 1993, Ruf et al, 1994). The quality of the retrieval relies on an accurate in-flight calibration, both in terms of absolute mean values and of time stability. To achieve this calibration, regular measurements of two known loads is performed, by switching the receiver either on an internal hot load (at ambient temperature) or on a sky horn, pointing to cold sky (cosmic background of 2.7 K and galactic noise).. However, the microwave circuit is different during calibration, since switches are used to connect the receiver to the calibration targets (contrary to scanning radiometers, for which the calibration targets are seen during the antenna rotation). The on-ground calibration procedure, based on measurements in a thermal / vacuum chamber, is not sufficient to ensure a good calibration, because (i) the reflector is not generally included in the chamber, because of its diameter, and (ii) the temperature range does not correspond to space conditions, since the lower temperature is the one of liquid nitrogen((77K). Another source of calibration uncertainty is the antenna itself : it is very difficult to properly estimate the radiation emitted by the various sources in space (including the satellite and earth), even a good characterization of the antenna pattern has been performed before launch. Finally the reflector quality is subject to degradation in space due to impacts with debris or other small particles.

CLS -	Final Report on activities performed in 2002-2004 on the ERS2/MWR survey	Page : 22 Date : 2004-12-10
Source ref : CLS-DOS-NT-04-255	Nomenclature : -	Issue : 1 rev. 0

For all these reasons, it is not possible to be fully confident in the pre-launch calibration adjustment, and careful analysis and correction is required after launch. Such analysis must moreover be repeated with time to ensure that no unknown effect has modified the instrument overall calibration.

In this paper, we present a comparative study of the calibration of the microwave radiometers on board the ESA Earth Remote sensing Satellite ERS2 and the NASA TOPEX. The radiometer characterization and performance analysis was achieved through pre-launch ground calibration and in flight calibration / validation (Ruf et al, 1995, Ruf et al, 1994, Eymard and Boukabara,1997). After TOPEX launch in 1992, the TOPEX Microwave Radiometer (TMR) has continuously been operated without any major failure, and the retrieved tropospheric correction is still within the initial specifications. One year after launch, the ERS2 Microwave Radiometer (EMWR) experienced an incident on one receiver, requiring a specific correction. Since this date, the radiometer performances have been slightly degraded (noise increase), but the tropospheric correction is still reliable and within the specifications. Comparisons of the two instruments were performed (Stum, 1998) at cross-over points of the satellite orbits, showing small differences between their respective calibration in the current brightness temperature range over ocean, as well as in the retrieved tropospheric corrections. In 2000, several careful analyses of the TMR time series led to establish a weak drift of the radiometer along its life (Ruf et al, 2000, Keihm et al, 2000).

The purpose of the present study is therefore to examine the absolute calibration of both radiometers along their life, using measurements over natural targets in the whole range of brightness temperatures. First we revisit the previous long term drift studies, by using a similar method for the two instruments, then we investigate the interest of continental targets to evaluate and compare the radiometer calibration at moderate to high brightness temperatures.

Section 2 presents both radiometers and their known problems. In section 3, the use of cold ocean analysis is discussed to point out long term trends on both instruments; in section 4, the use of stable continental targets is evaluated in complement for extending the brightness temperature range. Section 5 focuses on the comparison of absolute calibrations of both

CLS -	Final Report on activities performed in 2002-2004 on the ERS2/MWR survey	Page : 23 Date : 2004-12-10
Source ref : CLS-DOS-NT-04-255	Nomenclature : -	Issue : 1 rev. 0

radiometer, and explores in more details the use of the Amazon forest as a hot target to inter-calibrate microwave radiometers. Finally, conclusions are summarized in section 6.

2. The two radiometers : in-flight calibration results after launch

2.1 Radiometer specifications

The microwave radiometers are specified to provide the “wet” troposphere path delay with an uncertainty of 1 cm or lower, at the location of the altimeter footprint (any bias in the tropospheric correction directly impacts the sea level determination). In this aim, the TMR as well as the JMR (Jason radiometer) both have three channels, one below the water vapor line at 18 – 19 GHz (low sensitivity to clouds), one in the absorption line (21 - 23.8 GHz) and one in the 30 – 40 GHz band (as sensitive to the surface as the low frequency one, but more sensitive to cloud liquid water). The ESA ERS1/2 and ENVISAT radiometers do not include the low frequency channel. Due to this limitation, the tropospheric path delay retrieval is performed by using either the altimeter derived surface wind, or the backscattering coefficient in Ku band as a “third” channel (see Eymard et al, 1996, Tran et al, 2003). The table 1 summarizes the sensors and channels of the ERS2/ENVISAT and TOPEX/JASON missions. Note that the ERS1, ERS2 and ENVISAT radiometers have the same specifications.

The major specificity of these radiometers is the Dicke switch : the gain stability is ensured by switching at a high rate (1 or 2 kHz) between the main antenna and a reference load, and the actual measurement is the difference between the Dicke reference load temperature and the antenna temperature. In consequence, the sensitivity to major calibration errors is reduced at high brightness temperature (close to the instrument internal physical temperature) and maximal at low brightness temperature.

From on-ground calibration, the radiometer transfer functions (relation between the detected signal (voltage or digital count) and the brightness temperature) were established, and are used for the level 1 data processing (calibrated brightness temperatures), (see Bernard et al, 1993 and Ruf et al, 1994 for details concerning respectively ERS1 and TOPEX radiometers). Measurements in a thermal vacuum chamber were used to establish a preliminary set of calibration coefficients for all microwave elements. Antenna pattern measurements were

CLS -	Final Report on activities performed in 2002-2004 on the ERS2/MWR survey	Page : 24 Date : 2004-12-10
Source ref : CLS-DOS-NT-04-255	Nomenclature : -	Issue : 1 rev. 0

made in addition to complete the on-ground calibration. The absolute uncertainty was estimated from on-ground calibration, by evaluating all error sources within the radiometer (receiver, errors in loss coefficients, antenna characterization), and side lobe contribution errors, assuming they are not correlated. For both instruments, it was estimated to better or equal to $\pm 3K$. The radiometric sensitivity, derived from the time integration, bandwidth and noise temperature, was found to be lower or equal to 0.5K (see Ulaby et al, 1981, Skou, 1989 for more details about radiometer calibration)

After launch, the radiometer calibrations of both instruments had to be tuned, leading to significantly modify some calibration coefficients: any error in the characterization of microwave elements (loss factor, mainly) directly impacts the brightness temperature calculation, with an effect depending on the temperature gradients within the radiometer and with respect to the input antenna temperature. For this reason, any drift in the calibration, due to degradation of a microwave component (as for example a switch loss) should have the largest effect at the lowest observed temperatures. Due to the Dicke principle, it should be less detectable at high temperature than at low one.

2.2 In flight calibration : methods and results

For evaluating the in-flight calibration, the major difficulty is to find proper references. The methods currently used rely on comparisons between measurements of the instrument of interest and :

- measurements from similar instruments;
- measurements from ground based radiometers;
- simulations over sea using atmospheric profiles, sea surface temperature and wind, and a radiative transfer model ;
- combination of the two methods, by comparing simulations on the same meteorological fields with measurements from various other instruments (scanning radiometers as the Special sensor Microwave/Imager SSM/I on board the DMSP platforms or the TRMM Microwave Imager TMI. Main characteristics of these two instruments are given in Table 1).

CLS -	Final Report on activities performed in 2002-2004 on the ERS2/MWR survey	Page : 25 Date : 2004-12-10
Source ref : CLS-DOS-NT-04-255	Nomenclature : -	Issue : 1 rev. 0

An additional indirect way to control the in-flight calibration is to validate the retrieved products, the path delay in this case. This can be achieved by comparing it to the path delay derived from operational radiosonde profile measurements over ocean (from ships, small islands), by selecting satellite data falling in a time / space window centered on the radiosonde launch. Despite collocation error induced noise, any mean difference between path delays may be due either to the calibration of the radiometer or the radiosonde, or to the inversion method, and an empirical adjustment may be performed afterwards to fit the path delay with the required accuracy. Indeed, the radiosonde calibration uncertainty is a limitation for accurately determining the actual radiometer retrieval performance.

None of the above methods can ensure that brightness temperatures are calibrated with respect to an absolute reference, since the only observable reference is the cold sky. The use of such observations, by rotating the satellite, has occasionally been used for some radiometers, but this method ensures a good accuracy for the lowest temperature, not for the whole range. Consequently, the calibration of a new radiometer has generally to be tuned to previous sensors considered as a reference (ENVISAT radiometer on EMWR, itself calibrated on ERS1 radiometer (Obligis et al, 2004, Eymard and Boukabara, 1997), JMR on TMR as well, as proposed by Ruf et al, 2002). Nevertheless the continuity between missions, even crucial for altimeter missions in the context of a sea level rise survey at the millimeter level, does not justify neglecting technological and algorithmic improvements and may lead to artificial calibration errors on new instruments.

Algorithmic improvements have been related to the development of powerful non-linear statistical methods as neural network techniques, and the use of most reliable radiative transfer models. Errors due to direct simulations are now very small for the atmosphere radiative transfer (in non-rainy conditions), allowing to properly simulate operational atmospheric sounders, like those on board the operational meteorological platforms (Pardo et al, 1995, Garand et al, 2001). Sea surface emissivity models are more questionable, but their errors are within a few Kelvin (Eymard et al, 2000).

In the case of TMR, Ruf et al (1994) used a combination of various methods, by :

CLS -	Final Report on activities performed in 2002-2004 on the ERS2/MWR survey	Page : 26 Date : 2004-12-10
Source ref : CLS-DOS-NT-04-255	Nomenclature : -	Issue : 1 rev. 0

- (i) modeling the thermal behavior of the instrument as a function of internal temperature, as brightness temperatures had been found to vary by up to 10K with the solar heating;
- (ii) comparing measurements with those of ground based radiometers and other water vapor measurements, as well as with SSM/I brightness temperatures over the Amazon forest. From these comparisons, biases on the three channels were evidenced;
- (iii) re-analyzing and updating the on-ground calibration coefficient data set, and adjusting the antenna pattern characterization (account for side lobe contributions) to reduce the observed biases.

The resulting final calibration uncertainty was estimated to range within $\pm 1.5K$. In addition, the retrieval algorithm was improved, to fine tuning the path delay retrieval.

For EMWR (ERS and ENVISAT as well), the in-flight calibration consisted of:

- (i) comparing brightness temperatures from ERS2 with those of ERS1 (which was on the same orbit, with an half an hour time lag during the first months of ERS2)
- (ii) , comparing measured brightness temperatures with simulated ones, using collocated profiles from the European Centre for Medium Range Weather Forecasting (ECMWF) model analyses. A space-time threshold of respectively ± 0.5 degree and ± 30 minutes was taken, to statistically ensure the same air mass is considered in both cases, and cloudy points were removed using predicted liquid water content by the model and derived from EMWR using a retrieval algorithm (Eymard et al, 1996, Obligis et al, 2004). Any difference greater than 3K (estimated calibration uncertainty) was then removed by tuning internal parameters controlling the in-flight calibration calculation (mainly the sky horn and main antenna feed transmission coefficients) (Bernard et al, 1993, Eymard and Boukabara, 1997, Obligis et al, 2004). The relevance of this approach was

CLS -	Final Report on activities performed in 2002-2004 on the ERS2/MWR survey	Page : 27 Date : 2004-12-10
Source ref : CLS-DOS-NT-04-255	Nomenclature : -	Issue : 1 rev. 0

evaluated by performing similar comparisons on several radiometers, on the same ECMWF analyses (Eymard and Obligis, 2000).

- (iii) To ensure consistency between the instrument calibration for use of the retrieval algorithms (independently developed using an ECMWF data base and a radiative transfer model) , , a fine adjustment of radiometer coefficients was made, within the estimated absolute calibration uncertainty of $\pm 3K$. The final validation of path delays was achieved using shipborne radiosonde profiles.

The final uncertainties of path delay from TMR and EMWR were found to be less than 1cm and about 1cm, respectively.

2.3 Reported problems

2.3.1 *TMR*

The TMR did not experienced any noticeable anomaly. However, TMR was developed on the basis of a spear of the Scanning Multichannel Microwave radiometer (SMMR), which was flown on board SEASAT and NIMBUS7 satellites. The SMMR calibration was found to anomalously vary, due to temperature changes in the antenna. To overcome this problem, a radome was put to protect the main antenna and the sky horn and a specific correction was applied (Ruf et al, 1994). Nevertheless, small brightness temperatures biases were found between measurements during two satellite yaw modes (fixed or sinusoidal), An empirical correction was proposed by Callahan (2003).

Keihm et al. (2000) pointed out a drift of the TMR wet tropospheric correction with respect to SSM/I water vapor products and radiosonde measurements and they evaluated it to be $-0.2K/year$ drift in the 18GHz TMR brightness temperatures. In Ruf (2002), it was attributed to an increase of signal leakage from the warm calibration load to the radiometer antenna. More recent estimation of these drifts shows that, the drift did not stop in 1996 as first suggested by Ruf (2002), but continued until 1998 (Callahan, 2003).

2.3.2 *EMWR*

On 16 June 1996, a strong anomaly occurred on the 23.8 GHz channel. This anomaly was identified as a huge drop of the gain, which stabilized afterwards at approximately one tenth of its original value, leading to a decrease of about 10 K in brightness temperature. This

CLS -	Final Report on activities performed in 2002-2004 on the ERS2/MWR survey	Page : 28 Date : 2004-12-10
Source ref : CLS-DOS-NT-04-255	Nomenclature : -	Issue : 1 rev. 0

incident was identified as a possible failure of an amplifier in the receiver, and an empirical correction was proposed by Eymard and Boukabara (1997) after fitting brightness temperatures over polar regions (characterized by large range of temperatures, and a low day to day atmosphere variability) to those measured before the anomaly (just before and one year before the anomaly).

Stum et al (2001) pointed out a possible drift of the brightness temperatures measured by the EMWR at 23.8 GHz by analyzing the difference between ERS2 and TOPEX wet tropospheric corrections and brightness temperatures at cross-over points. The drift was confirmed and quantified later on (Eymard et al (2002), Obligis et al (2004) and Sharroo et al (2004)). The mean value for this drift was estimated to be -0.2K/year corresponding to a wet tropospheric correction about 5 mm lower 7 years after launch.

On both radiometers, the small trend detected could be due to aging effect on switches, as suggested by Ruf (2002) for TMR. Empirical functions depending on brightness temperature and time were proposed by Ruf (2000)and, Obligis et al (2003) to correct for the respective drifts of each radiometer.

3. Long term calibration analysis of the two radiometers over “cold” Ocean

3.1 Coldest brightness temperatures over ocean

Because of the several independent analyses that established that the TOPEX radiometer (TMR) had drifted with time (implying a trend on the retrieved path delay), Ruf (2000) developed a method to evidence and monitor the drift of any of the three channels. Modeling considerations gave the order of magnitude of the minimum value, which could be measured over the ocean (cold water, specular reflection due to no wind and dry atmosphere conditions). A threshold was then derived from these values (minimum + 10 K) to select data within each TOPEX cycle. The resulting brightness temperatures histogram were then plotted and fitted with an third order polynomial function, that allowed extrapolation and determination of the minimum brightness temperature value. Time series of these minimal temperatures for the three channels exhibited a significant difference in behavior between the 18 GHz channel and the others, confirming the drift on the 18 GHz channel . The obtained 18

CLS -	Final Report on activities performed in 2002-2004 on the ERS2/MWR survey	Page : 29 Date : 2004-12-10
Source ref : CLS-DOS-NT-04-255	Nomenclature : -	Issue : 1 rev. 0

GHz channel trend is 0.27 K per year over the first 5 years (until the end of 1996), and a slightly lower rate since then.

In Ruf's method, the three channels are processed independently, so the selected data from each channel used to derive the minimal temperature do not coincide in space / time. To check the possible importance of analyzing the same data sets on the 3 channels, we developed a method derived from Ruf's one. Similarly, coldest measurements were first selected by selecting data below Ruf's lowest threshold +10 K, but in our case for all channels together. Then the mean and standard deviation of the remaining data of each cycle were computed, and finally, only data falling below the mean minus 1.5 times the standard deviation, were plotted. The same method was applied to both TMR and EMWR.

The figures 1-a and 1-b show the results obtained for TMR and EMWR respectively. For TMR, Ruf's results are confirmed with a slightly lower trend : the 18 GHz trend is here of 0.21K/year over the 7 first years (1992 – 1999), and seems to decrease within the last two years (0.17K/year when considered over 9 years). The 21 GHz channel is stable with time (0.012 K/year over 7 or 9 years) whereas a small trend is possibly significant on the 37 GHz channel (0.04 K/years over 7 or 9 years).

As the TMR 18 GHz channel, the suspected EMWR 23.8 GHz channel drift is confirmed, the total decrease being -0.27K/year over 6 years, whereas the 36.5 GHz has remained rather stable (0.03K/year) over the same period. Note that the first year of ERS2 radiometer data were not included in this analysis, because of the failure mentioned previously : any small error in the empirical correction of the gain drop was shown to induce artificial drift with respect to the first year. We analyzed the data set linearly corrected for the reported gain anomaly.

3.2 Cross-over comparisons

The above method allows an absolute determination of a drift for each particular channel. However, the uncertainty of the drift is difficult to evaluate (e.g. the difference between Ruf's results and ours). To confirm the robustness of the method, cross-over points between TOPEX and ERS2 orbits were used. The TMR 21 GHz channel, identified as the most stable in the previous section, was taken as a reference to select the coldest points. Again, a

CLS -	Final Report on activities performed in 2002-2004 on the ERS2/MWR survey	Page : 30 Date : 2004-12-10
Source ref : CLS-DOS-NT-04-255	Nomenclature : -	Issue : 1 rev. 0

threshold was applied to the 21 GHz brightness temperatures, and only those data, which were collocated with these selected 21 GHz TBs, were plotted. The collocation processing selects the EMWR and TMR closest measurement within a +/- 1 hour common window around each orbit cross-over point. Figures 2-a and 2-b show the resulting plots for TOPEX and ERS2 brightness temperatures at each frequency respectively. The trends are of the same order of magnitude but slightly different from those obtained with the previous method (values of the trends obtained with the two methods are given in table 2). This is mainly due to the different spatial distribution, since cross-over points between ERS2 and TOPEX are located at high latitudes. The number of cross-over locations (a few hundreds) as well as their geographic distribution being limited, the uncertainty on the trend is higher than the one of coldest ocean data (previous section) and possibly not fully representative.

Figure 3 shows the impact of these drifts on the ERS2 and TOPEX wet tropospheric corrections at cross-over points. They both are less than 1mm per year, showing that the two instruments are very stable over their life, despite their respective drifts.

3.3 Discussion

In Table 2 are reported the drifts obtained using the above methods. Ruf's TMR 18GHz drift is also given, and those recently estimated by Scharroo et al, using another method close to Ruf's one, but slightly different: the coldest value of each cycle is derived from a linear extrapolation of the cold data histogram, taking the lowest 0.5 to 1% number of points.

For the TMR 18 GHz channel, the estimates of Ruf, Scharroo, and the one obtained in section 3.1 are consistent and close to each other within +/-0.03 K/year. The cross-over analysis leads to a smaller drift. There is no drift estimate for the other channels in Ruf's study. The results obtained in the present study are consistent with each other, and with Scharroo's results. They all conclude to very weak drifts, probably not significant on both channels. Concerning EMWR, consistent results on the 23.8 GHz channel are again observed between our study and Scharroo's one (negative drift of about 0.1 to 0.27 K/year). The 36.5 GHz channel has a similar stability as the TMR 37 GHz one. The discrepancy between estimates gives an evaluation of the confidence on the drifts: an uncertainty of 0.05 to 0.07 K/year is consistent

CLS -	Final Report on activities performed in 2002-2004 on the ERS2/MWR survey	Page : 31 Date : 2004-12-10
Source ref : CLS-DOS-NT-04-255	Nomenclature : -	Issue : 1 rev. 0

with all estimates. This means that those drifts, which are smaller than 0.07 (on the TMR 21 and 37 GHz, and the EMWR 36.5 GHz channels) are probably not significant.

As mentioned in section 2, the drifts evaluated at low temperature are the highest, because of the Dicke technique, so the average drift values at brightness temperatures usually measured over ocean are smaller. In the next section, we will analyze the radiometer stability over selected “hot” and “cold” continental areas, to complement this analysis at higher brightness temperatures.

4. Stability analysis on stable continental areas

Continental areas are generally not used to check radiometer calibration, because of the high and very variable emissivity of the land surface. However, there are a few locations over the globe, where the atmosphere conditions and/or surface emissivity stability are sufficient to envisage such use. In this section, we test this approach to check the long term drift of every channel at various temperatures.

4.1 Selection of continental targets

Criteria to select continental areas were the maximal horizontal homogeneity and a small time variability of the surface. One year cycle of ERS2 radiometer measurements was explored, and various areas were investigated. Three “cold” and two “hot” areas were thus selected (see Table 3). The “cold” areas are located over the Antarctic plateau, far from the coast, close to the limit of the field of view of the instrument due to the orbit inclination (82° in latitude), at an elevation of about 2000m. Snow fall occur each winter, and the wind is weak. The third “cold” area is located on the Greenland plateau, as North as possible but within the TOPEX orbit overpass. The average brightness temperature is close to the mean value over ocean. One of the “hot” area is in the Sahara desert (East Mauritania). The surface is very dry (no rain) and sandy. The last area is located in the Amazon forest, far from coasts, and from mountains. Here the surface is covered with a dense vegetation, crossed by rivers.

Their size is small enough to assume horizontal homogeneity, except for specific elements which were removed (mainly a river in the NW corner of the Amazon forest area), but they contain at least one orbital « node » of both missions.

CLS -	Final Report on activities performed in 2002-2004 on the ERS2/MWR survey	Page : 32 Date : 2004-12-10
Source ref : CLS-DOS-NT-04-255	Nomenclature : -	Issue : 1 rev. 0

All these areas, except the Amazon forest one, are characterized by a dry to very dry atmosphere throughout the year, so the temporal variations mainly come from surface temperature and surface emissivity variations. The Amazon forest was added because it has been shown that dense forest is the natural target which is the closest to a natural blackbody (Ruf et al, 1994, Brown et al, 2004). In addition, the high mean temperature leads to a maximal emission in the microwaves, so the highest brightness temperatures over the globe.

Over the five areas, we analyzed the long term trends, as well as mean values. Except for Amazon forest, the effect of the water vapor is weak, so the mean brightness temperatures should mainly vary with the emissivity of each area, for a given surface temperature.

4.2 Analysis method

Over each orbit segment over-passing the selected area, the mean and standard deviation of the brightness temperatures were computed. The resulting ERS2 time series (23.8 GHz channel) are plotted over each area in Figure 4. Before analyzing time series from each channel and for every area, specific aspects, linked to the natural variations of the surface emissivities, had to be examined :

(i) the diurnal cycle

The diurnal cycle has an important effect over Sahara and Amazon forest. To take into account the variations of the surface temperature due to the diurnal cycle, the over-passing local solar time is considered. The Figure 5 shows the average diurnal cycle of TMR brightness temperatures, over one year in the Amazon forest area. Contrary to the TOPEX mission, the ERS2 is in sun-synchronous orbit, crossing the equator at 10 am and 10 pm (local solar time). TMR data were thus selected at the same overpass time as EMWR for each area, within +/- 1 hour.

(ii) the annual cycle

The annual cycle strongly dominates the signal over Sahara and Antarctic areas. To evaluate the trend, an entire number of solar cycles was considered. As the solar cycle masks other possible variability modes, a low-pass filter was also applied. Over the Antarctic plateau, an

CLS -	Final Report on activities performed in 2002-2004 on the ERS2/MWR survey	Page : 33 Date : 2004-12-10
Source ref : CLS-DOS-NT-04-255	Nomenclature : -	Issue : 1 rev. 0

inter-annual variability was observed period of about two years), which could influence the drift estimate.

(iii) the ice melting

Over the Greenland area, the difficulty mainly comes from the huge variation of the brightness temperatures due to summer melting. The contaminated data were eliminated by computing, for every annual cycle, the mean and standard deviation of brightness temperatures, then by removing those which are higher than the mean plus 0.5 times the standard deviation (see fig.4). This method is derived from the one developed by Torinesi et al (2003), to identify the melting signal on SSM/I data over the Antarctic coastal boundary.

4.3 TMR and EMWR trends over continental areas

The difference between night and day temperatures made necessary to separate the corresponding overpasses over Sahara and the Amazon forest.

Table 4 summarizes the results of the EMWR survey over 6 years. We did not include the first year, for the same reason as for ocean coldest point analysis. The first result is that the trends are different from one area to another. Even over the Antarctic plateau, positive trends are found on the first area for both channels, whereas the trends are negative on the second one. The natural interannual variation of each area is most likely the main cause of this discrepancy. However, when considering the relative trend (channel 36.5 – channel 23.8), a significant difference appears:

it is positive over coldest targets (Antarctic plateau), close to zero over Greenland, and it is negative over warm areas (Sahara and Amazon forest). The positive relative trend for cold targets is consistent with the analysis over ocean (negative trend on the 23.8 GHz channel). The result over “hot” targets suggests that the relative trends are inverted (increase of the 23.8 GHz channel relative to the 36.5 one).

A similar analysis was performed on TMR data (Table 5). Over Greenland, a slightly negative trend is observed for the difference between trends at 21 and 18 GHz (0.04 K/year). The other relative trends between the 21 and 18 GHz channels are negligible. The relative

CLS -	Final Report on activities performed in 2002-2004 on the ERS2/MWR survey	Page : 34 Date : 2004-12-10
Source ref : CLS-DOS-NT-04-255	Nomenclature : -	Issue : 1 rev. 0

trend between 37 and 21 GHz over hot targets is slightly positive (except over Amazon forest during night).

The signs of the relative trends of EMWR and TMR over cold continental targets are consistent with results of the cold ocean analysis, but the absolute trend on each channel cannot be derived from time series over continental areas, because of the natural interannual variability of each of them. Larger data sets should probably be necessary to reduce this effect, particularly over Greenland.

Over hot targets, the result for EMWR indicates also a trend, but different from the one at low temperature. Such a trend could possibly exist on TMR high values, but the small number of data per cycle makes the estimate rather inaccurate.

Such a trend at high temperatures, if it is confirmed, will require further analyses of the in-flight calibration.

5. Comparison of TMR and EMWR absolute calibrations

5.1 EMWR-TMR comparison of mean brightness temperatures over continental targets

The interest of selecting the same areas for TMR and EMWR is that a direct comparison of the measured brightness temperatures is possible, assuming that the surface emissivity does not significantly vary at frequencies close to each other. Estimates of the land surface emissivity using SSMI (Prigent et al, 2000) and AMSU-A (Karbou et al, 2004) in the range 18 – 89 GHz validate this assumption: in case the atmospheric absorption does not contribute for a large fraction in the measured brightness temperature, measurements at frequencies as close as 18, 21, 23.8 GHz can be quantitatively compared, as well as measurements at 36.5 and 37 GHz. Table 6 shows intercomparison results on the 3 selected areas, Greenland, Sahara and Amazon forest (the assumption is less valid in the latter case). Data are averaged over the 7 common years, now neglecting the respective drifts of both instruments (the mean error on brightness temperatures, assuming that the trend is a linear function of brightness temperature, is -0.7K for TMR 18 GHz and $+0.8\text{K}$ for EMWR 23.8 GHz channels. In the following, we will neglect this error, considering the overall absolute calibration uncertainty (2 – 3K).

CLS -	Final Report on activities performed in 2002-2004 on the ERS2/MWR survey	Page : 35 Date : 2004-12-10
Source ref : CLS-DOS-NT-04-255	Nomenclature : -	Issue : 1 rev. 0

The comparison between TMR and EMWR reveals a similar behavior over Greenland (less than 2K between the 21/23.8 GHz and the 36.5/37 GHz channels), despite the slightly different frequencies.

Over Sahara and Amazon forest, the difference between the 21 and 23.8 GHz channels is 6 – 7K, and it is 12-13K for 36.5/37 GHz channels, which should be nearly similar !

Over Greenland, brightness temperatures are in the range of those obtained over ocean. Most of the in-flight calibration / validation effort were made to optimize data in this range. At high temperature, Ruf et al (1994) included comparisons with SSM/I, but on a limited data set, and no calibration comparison was performed in this range for EMWR. In the literature, the question of in-flight calibration of microwave radiometers is rarely developed, and no indication could be found on high temperatures for other instruments.

Thus, contrary to low temperatures, for which modeling and path delay validation may be used to check the instrument absolute calibration, no method has yet been established to assess the calibration in the upper range. The question that arises is which reference could we use to analyze the calibration of both sensors at high temperatures?

5.2 AMSU-A brightness temperatures as a common reference over the Amazon forest

To address this question, we chose to focus on the Amazon forest, as the deep forest is the closest to a natural blackbody for the microwave range. This area presents small vertically and horizontally polarized TB difference (mean is approximately less than 1 K) as measured by the SSM/I radiometer at its two window channels at 19.35 and 37.0 GHz (Brown and Ruf, 2004), which characterizes regions with high atmospheric opacity and an optically thick vegetation canopy. The measured TBs are weakly dependent on frequency (the surface temperature seen by the sensors is only slightly frequency dependent due to the difference in penetration depths into the medium, and the atmosphere contribution is stable). Nevertheless, the TOPEX and ERS orbits do not cross each other often enough to guarantee the statistical consistency of direct comparisons, except by averaging data over several years, as we did in the previous section. We could use SSM/I, as did Brown and Ruf (2004), but this requires an empirical function for transposing measurements at 53 degrees of incidence to nadir looking. Another scanning instrument of interest is AMSU-A.

CLS -	Final Report on activities performed in 2002-2004 on the ERS2/MWR survey	Page : 36 Date : 2004-12-10
Source ref : CLS-DOS-NT-04-255	Nomenclature : -	Issue : 1 rev. 0

AMSU-A provides a high spatial and temporal sampling of the Earth's surface for a large range of frequency and has two window channels (at 23.8 GHz and 31.4 GHz) near those used on altimeter missions (see table 1). Moreover two field-of-views (fov) are at near nadir local zenith angle ($1^{\circ}40$ and $-1^{\circ}40$) so the measurements are directly comparable with radiometers TBs on altimeter missions. AMSU-A is dedicated to temperature profiling through assimilation into weather forecasting models. AMSU-A on-board calibration is performed by viewing the cold space background with the same antenna every 8 seconds for each scan line. Thanks to the transverse scanning of AMSU-A reflector, it is possible to compare AMSU-A and SSM-I data (at 53 degrees incidence), by combining the SSM/I H and V polarizations to get the exact AMSU-A one. Karbou et al (2004) thus checked the consistency between both instruments, with results within less than 0.5K for most channels over land (desert, dense forest). Regarding all these points (regular complete internal calibration, 2 views close to the nadir point, frequencies near those of altimeter missions), the AMSU-A brightness temperatures can be considered as a reliable relative reference.

Nevertheless, the calibration assessment for each instrument has to account for contributions in the side lobes of the antenna before comparison of the brightness temperatures:

- In SSM/I case, the incidence angle is constant, but, within the antenna rotation, radiating elements such as a solar panel could bias the measurement for some scanning position. Corrections for the antenna sidelobes were verified by aircraft underflights with an SSM/I simulator (Ruf et al, 1994), making one confident on the SSM/I calibration.
- The side lobe correction (due to earth contribution) for EMWR is based on the main lobe measurement: there is therefore no added bias when the measurement is taken far from the coasts (Eymard and Boukabara, 1997).
- The TMR side lobe correction was tuned over ocean (Janssen et al, 1995), where the brightness temperatures in the side lobes are lower than over the Amazon forest. A negative correction should therefore be added to TMR data to correct them for land surface side lobe contribution.

The AMSU-A transverse scanning reflector requires a careful analysis of the side lobe contributions, because contribution from the earth is maximal at nadir, then decreases as the

CLS -	Final Report on activities performed in 2002-2004 on the ERS2/MWR survey	Page : 37 Date : 2004-12-10
Source ref : CLS-DOS-NT-04-255	Nomenclature : -	Issue : 1 rev. 0

incidence angle increases up to the limb view. Mo et al (2001) proposed a calibration correction function of incidence angle. No information could be found on any surface type dependent correction for AMSU-A.

5.3 Comparison of AMSU-A, TOPEX and ERS2 brightness temperatures over the Amazon forest

AMSU-A measurements for one full year, 2002, have been used, over the Amazon forest area (table 2). The scan pattern and geometric resolution correspond to a 40 km diameter cell at nadir. Since the NOAA-16 is in a circular sun-synchronous near-polar orbit, the selected area is over-flown twice a day at respectively around 02:00 local solar hour (LST) and 14:00 LST.

Measurements were taken during the day time and night time passes to evaluate the stability of the brightness temperatures. Channels 23.8 and 31.4 GHz were studied, as they are the closest in frequency from TMR and EMWR ones. The TBs from fovs 15 and 16, closest to the nadir view, have average values greater than 280 K and standard deviations of less than 2 K, as summarized in Table 7. A small increase in the mean TB is evident from nighttime to daytime. Both nighttime and daytime TBs were found to be quite stable values over the four seasons. The variation over seasons and the standard deviation at night tend to be less than those in the day time hours. For this reason the nighttime data will serve as a reference over this area to compare the different sensor brightness temperatures.

We compared the brightness temperatures from TMR and EMWR versus AMSU-A. SSM/I data were also included for comparison with the previous study of Brown and Ruf (2003). We used their algorithm to recompute the SSM/I TBs into a vertical incidence configuration. We limited our comparison for TMR to time intervals close to AMSU-A overpasses. Note that the SSM/I instrument on DMSP F-13 over-flies the area between 05:00 and 07:00 LST while AMSU-A precedes it at around 02:00 LST, and this difference in viewing time could lead to a few tenths of K in difference with lower values at dawn hours, as shown on the average TMR diurnal cycle plot (Figure 4). Due to the different overpass time of the sun-synchronous satellites, we must limit this comparison to early hours, to minimize the effect of the diurnal cycle: the differences could reach up to 4 K between dusk and dawn. A difference of 1-2 K

CLS -	Final Report on activities performed in 2002-2004 on the ERS2/MWR survey	Page : 38 Date : 2004-12-10
Source ref : CLS-DOS-NT-04-255	Nomenclature : -	Issue : 1 rev. 0

would therefore be normal to observe between nighttime TB measurements of AMSU-A and ERS2 ones.

Average brightness temperatures over the nighttime hours are displayed in Table 8. TMR exhibits the smallest values at all its frequencies. All reported 23.8 GHz measurements are in good agreement (AMSU-A, EMWR, and SSM/I (extrapolated at nadir). The EMWR 36.5 GHz provides a too high value at 291.9 K. Except for this latter, we observed the overall slight decrease of TB with increasing frequency. The standard deviation ranges between 1.0 and 2.8K, giving a good confidence in the mean values.

External causes of discrepancy could be:

- the difference in frequency between channels compared (31 to 37 GHz, 18 to 23,8 GHz), but this would mean a significant difference in emissivity between these channels, in contradiction with results obtained by Prigent et al (2000) and Karbou et al (2004)
- differences in local measurement time, which can lead to 6 K variation, but was minimized by taking night hours only (less than 2K variation). Effects of atmosphere variations (different atmosphere attenuation due to water vapor, clouds and rain) could also contribute to the discrepancy.
- Finally the horizontal heterogeneity of the area (the TMR and EMWR overpasses occur on specific portions of the area, different of each other, and possibly different from the global average, as seen by AMSU-A and SSM/I

To further analyze this hypothesis, we must reduce the errors due to external factors. In the next section, we propose a new method, based on the calculation of the surface emissivity in each channel of each instrument, in order to remove most of these unknown external effects.

5.4 Comparison of surface emissivities

Prigent et al. (1997, 1998) estimated the microwave land emissivity over the globe from SSM/I at the frequencies 19, 22, 35 and 85 GHz, for vertical and horizontal polarizations, at 53° zenith angle by removing the atmosphere, clouds, and rain contributions using ancillary satellite data. The well known simplified radiative transfer equation for one channel (stratified isothermal atmosphere) can be written as:

$$T_b = T_{up} + T_s e^{-\Gamma} + (1-e^{-\Gamma}) T_{down} \quad (1)$$

CLS -	Final Report on activities performed in 2002-2004 on the ERS2/MWR survey	Page : 39 Date : 2004-12-10
Source ref : CLS-DOS-NT-04-255	Nomenclature : -	Issue : 1 rev. 0

Where **T_{up}** is the upwelling radiation (from the atmosphere), **T_{down}** the downwelling radiation, including the galactic background, **Γ** the atmosphere transmittance, **T_s** the surface temperature and **e** its emissivity,

Providing **T_s** and atmosphere profiles, it is possible to derive **e** from **T_b** measurements. Following a similar approach, Karbou et al. (2004) estimated the AMSU-A land surface emissivities for 30 observation zenith angle ranges (from -58° to +58°) and for the 23.8, 31.4, 50.3 and 89 GHz channels, over January to August, 2000. Collocated visible/infrared satellite measurements from ISCCP (International Satellite Cloud Climatology Project) data have been used to screen for clouds and to provide an accurate and independent estimate of the skin temperature (Rossow and Schiffer, 1991). The nearby temperature-humidity profiles from ECMWF forty years re-analyses (ERA-40) (Simmons and Gibson, 2000) have been used as input to an updated radiative transfer model in order to estimate the atmospheric contribution to the measured radiances. AMSU-A emissivities have been evaluated by analyzing their variations with surface types, the observation angle, and the frequency. AMSU-A emissivities have been also compared to SSM/I ones previously calculated by Prigent et al, 1998.

When sorted by observation zenith angle and by vegetation type, the AMSU emissivities show rather strong angular dependence over bare soil areas. The emissivity angular and frequency dependence is found limited over areas with high vegetation density. The deep forest emissivity was shown nearly constant with incidence and frequency with possibly a small decrease by 2% between 23.8 and 89GHz, and a weak seasonal variability was found (less than 1%). For the 23.8 and 31.4 GHz channels, the emissivity calculations are as accurate as required for atmospheric applications; the day-to-day emissivity variation within a month is less than 2% (English, 1999 found that an accuracy of 2% is requisite for humidity profiles retrieval over land surfaces).

For AMSU-A, TMR and EMWR instruments, emissivity for each channel was calculated in a grid of 0.5x0.5 square degree meshes. At the studied frequencies, high thin ice clouds have a negligible impact on T_bs observations. However, for an optimum accuracy of the emissivity estimates, only cloud free data have been selected. The previously selected area in the

CLS -	Final Report on activities performed in 2002-2004 on the ERS2/MWR survey	Page : 40 Date : 2004-12-10
Source ref : CLS-DOS-NT-04-255	Nomenclature : -	Issue : 1 rev. 0

Amazon forest was found too small to ensure a sufficient number of cloud free observations over a short period of time (to limit the seasonal variation impact). Consequently, this area was extended to the entire deep forest in South America. The vegetation identification was performed using a vegetation classification (Dickinson et al, 1986) available at 30 km resolution (Figure 7). Data from January 2000 were used for emissivity comparisons. For adequate comparisons between microwave instruments, only AMSU data close to nadir (less than +/-10 degrees incidence) were taken.

AMSU-A mean emissivity maps over the Amazon forest as well as EMWR and TMR ones reveal geographical heterogeneities due to the rivers inside the forest (emissivity lower than the forest one), which are associated with rather low emissivities and high emissivity variability. River data were removed using thresholds applied at each grid mesh on both mean emissivity and on the associated standard deviation (when a portion of orbit fails in the grid mesh, the variation due to a river leads to a higher standard deviation): the chosen minimum mean emissivity is 0.9, and the maximal standard deviation is 0.03.

Figure 8 shows the obtained maps after this selection performed. A residual “contamination” by rivers is likely in some locations. However, a negligible effect is expected on the average emissivity values. The AMSU-A standard deviation map looks slightly more “noisy” than EMWR and TMR. This could be explained by larger AMSU-A footprint than TMR and EMWR ones, and the cloud filtering is less stringent since cirrus clouds were kept.

Before comparing the mean emissivities, three preliminary analyses were performed to check the reliability of emissivity calculations:

- Emissivity distributions for the three instruments are similar and close to a Gaussian shape, except for a mean bias (not shown) ;
- the emissivity time evolution within the month (daily means computed over the area) is flat, with no in the standard deviation change (not shown);
- the diurnal cycle (figure 9) exhibits a remaining variation for TMR, which is the only instrument for which emissivities are computed in the middle of the day and afternoon. The higher values obtained, compared with night time emissivities, suggest a likely bias in the day/night surface skin temperature or a wrong daily cycle of the ECMWF profiles.

CLS -	Final Report on activities performed in 2002-2004 on the ERS2/MWR survey	Page : 41 Date : 2004-12-10
Source ref : CLS-DOS-NT-04-255	Nomenclature : -	Issue : 1 rev. 0

Table 9 gives the January averaged emissivities over the entire zone, as well as the associated standard deviation. SSM/I emissivities, as calculated by Prigent et al (2000), are given for comparison (values for an equivalent AMSU polarization, at 18.7 and 37 GHz). All standard deviation are close to 0.02, and the emissivities range between 0.851 and 0.972. AMSU-A / SSM/I emissivities are consistent within the 2% uncertainty, and they show a slight emissivity decrease as noted above (by 0.02 between 18.7 and 37 GHz).

With respect to the AMSU-A / SSM/I mean values, TMR emissivities are lower (particularly at 18 and 21 GHz), and the EMWR 36.5 GHz channel one is higher. For these three channels (TMR 18 / 21 and EMWR/36.5), the calculated emissivity differ by more than 2% from the mean AMSU-A value, this discrepancy being thus larger than expected from any external cause.

In conclusion, comparisons over the Amazon forest both in brightness temperature and emissivity confirm the anomalous discrepancy between radiometers in the 21 – 37 GHz range, and suggest that these discrepancies are due to after launch calibration adjustments, since the latter method reduces the impact of external effects.

The causes of this calibration discrepancy should be analyzed separately for each instrument. A first error source is the difference in side lobe contributions : in section 5.1, the different processing methods for TMR and EMWR were found different. However, any error of 20K on the mean side lobe would lead to a bias of less than 1K on the brightness temperature, assuming a 3% contribution. Side lobe contribution differences therefore cannot be the unique source of discrepancy.

In section 2, in-flight calibration methods for TMR and EMWR were compared. At high values, no efficient validation could be performed, because high temperatures over oceans are observed in deep clouds and over sea ice, whereas the brightness temperature comparisons and path delay validations were performed over open ocean, preferably in clear air. Thus the temperature range of the in-flight calibration / adjustment procedure was limited to the low – medium range of brightness temperatures.

The procedure used by Ruf et al (1994) for adjusting the calibration in the high values consisted to fit TMR data to SSM/I measurements, after correcting the latter for incidence

CLS -	Final Report on activities performed in 2002-2004 on the ERS2/MWR survey	Page : 42 Date : 2004-12-10
Source ref : CLS-DOS-NT-04-255	Nomenclature : -	Issue : 1 rev. 0

angle and frequency, based on modeling considerations. Concerning EMWR, Eymard and Boukabara (1997) did not specifically adjust the high temperatures within the calibration correction procedure. The method used for tuning the in-flight calibration was indeed unable to correct for calibration anomalies at high temperature, as mentioned in section 2, and the cause for these anomalies, both on TMR and EMWR, are unexplained.

This explains that the biases at high temperature on EMWR 36.5 GHz and TMR 18 and 21 GHz channels were not detected, as long as nobody carefully looked at continental targets. Moreover, similar errors on SSM/I and AMSU-A could exist as well! The question of an absolute reference is therefore open for calibrating microwave radiometers in the whole range.

6. Conclusion and perspectives

In this study, we addressed the problems of the in-flight calibration of microwave radiometers over their life, and over the whole temperature range. We compared TOPEX and ERS2 radiometers, as they can be compared over a 7 years common interval.

In a first step, we revisited Ruf's method for determining the long term drift of TMR, by processing the three channels together, with a slightly simplified method. Consistent results were found, which confirmed the 18 GHz channel drift and showed the good stability of the 21 GHz channel. The same method, applied to EMWR, revealed a drift on the 23.8 GHz channel, but a good stability of the 36.5 GHz one. Cross-track comparisons confirmed again these results, and allowed to evaluate the drift impact on the wet tropospheric path delay in both cases. With respect to initial specifications, both radiometers are still compliant. However, these drifts must be compensated for to ensure the best accuracy, particularly for estimation of the long term sea level variation. In both cases, a linear correction (function of time and of temperature) has been proposed to date.

To enlarge the inter-comparison of TMR and EMWR calibration drifts, we examined the relevance of stable continental targets. On "cold" targets, as the Antarctic plateau and South Greenland, consistent trends with time were observed, but only in a relative manner (difference between brightness temperatures of two channels). On "hot" targets, as Sahara

CLS -	Final Report on activities performed in 2002-2004 on the ERS2/MWR survey	Page : 43 Date : 2004-12-10
Source ref : CLS-DOS-NT-04-255	Nomenclature : -	Issue : 1 rev. 0

and Amazon forest, no drift could be detected. As the two radiometers use a Dicke switch, calibration errors due to bad estimates of transmission / losses of any switch (and their drift) are maximal for low brightness temperatures (maximal difference with the internal temperature).

In a second part, the absolute calibrations of both radiometers were compared over stable continental areas. Over Greenland, measurements from TMR and EMWR were found consistent, within 2 – 3 K. However, “hot” targets revealed anomalously large differences between the two radiometers for both couples of frequencies (21 / 23.8 and 36.5 / 37 GHz). To further check the cause of this discrepancy, two successive comparisons were performed with AMSU-A and SSM/I corresponding channels. The advantage of AMSU-A is that its transverse scanning mode provides direct comparison at the same incidence angle with TMR and EMWR at nadir, and with SSM/I at 53 degrees.

- A direct comparison of TMR, EMWR, AMSU-A and SSM/I brightness temperatures over one year for the same area in the Amazon forest evidenced a “warm” bias on the EMWR 36.5 GHz, and suggested a “cold” bias on TMR channels. But different orbit characteristics (overpass time) and external effects (diurnal cycle of surface and atmosphere variations) could be partly cause of these discrepancies ;
- A comparison of derived land surface emissivities for the same channels was performed to remove all external error sources, using ancillary informations from ISCCP for cloud clearing and surface temperature, and ECMWF re-analyses for atmosphere profiles. The “warm” bias on EMWR 36.5 GHz was again evidenced, with respect to SSM/I and AMSU-A derived emissivities. Looking at the frequency variation of emissivity (stable or slightly decreasing with frequency, from AMSU-A and SSM/I data) suggests that TMR 18 and 21 GHz are biased “cold”, as the corresponding emissivity is about 3% lower than those of other sensors.

Such error in high brightness temperatures might be due to the in-flight calibration procedure, which generally relies on ocean data, thus in the low – medium range of brightness temperatures. Nevertheless, the absolute calibration of a radiometer is not necessary to

CLS -	Final Report on activities performed in 2002-2004 on the ERS2/MWR survey	Page : 44 Date : 2004-12-10
Source ref : CLS-DOS-NT-04-255	Nomenclature : -	Issue : 1 rev. 0

guarantee a good wet tropospheric correction retrieval. In fact, it is the consistency between calibration and retrieval methods, which will assure the quality of the product.

The use of stable targets is therefore complementary to cold ocean, not only to validate the instrument in-flight calibration but also to reduce the effects of time lag, for inter-comparison between measurements from different sensors. The tropical forest appears as a reliable target for such analysis, and the closest to a blackbody, but the use of other areas, as deserts could also being investigated.

It would be interesting to generalize this use of continental warm targets to systematically compare microwave radiometers after launch. It will not provide an absolute reference to which to fit measurements, but it might be a common relative reference to be used, in complement of other methods to ensure a better consistency of measurements from all microwave radiometers.

Acknowledgments:

The authors are grateful to the reviewers, who made fruitful suggestions for improving the paper. They would acknowledge Michel Dedieu, for his considerable help for data processing. This work was supported by CNES, (contract CNES/CLS 731/CNES/00/8435/00 and ESA(contract 16971/03/I-OL).

References :

- Bernard R., A. Le Cornec, L. Eymard and L. Tabary, The microwave radiometer aboard ERS-1, Part 1 : characteristics and performances, IEEE Trans. Geosci. Remote Sensing, 31, 6, 1186 - 1198, 1993.
- Brown S., C. Ruf, S. Keihm and A. Kitayakara, Jason Microwave Radiometer Performance and On-orbit Calibration, Marine Geodesy, 27, 199-220, 2004.

CLS -	Final Report on activities performed in 2002-2004 on the ERS2/MWR survey	Page : 45 Date : 2004-12-10
Source ref : CLS-DOS-NT-04-255	Nomenclature : -	Issue : 1 rev. 0

Callahan P. S., User notes for revised GDR correction product (GCPB), Tech. Note to the TOPEX/Poseidon/Jason Science Working Team, Jet Propulsion Laboratory, California Institute of Technology, Pasadena, California, 2003.

Dickinson, R. E., A. Henderson-Sellers, P.J. Kennedy, and M.F. Wilson, "Biosphere-atmosphere transfer scheme (BATS) for the NCAR community climate model," NCAR Technical Note NCAR/TN275+STR, Boulder, CO. 69 p, 1986.

English, S., 1999, Estimation of temperature and humidity profile information from microwave radiances over different surface types, *J. Appl. Meteorol.*, vol. 38, pp. 1526-1541.

Eymard L. and S.-A. Boukabara, Calibration – Validation of the ERS2-2 microwave radiometer, Final Report of European Space Agency Contract 11031/94/NL/CN, 1997.

Eymard L., A. Pilon, E. Obligis and N. Tran, Intercomparison of TMR and ERS/MWR calibrations and drifts, Jason-1/TOPEX/Poseidon Science Working Team Meeting, 21-23 October 2002, New Orleans, 2002.

Eymard L., L. Tabary, E. Gérard, A. Le Cornec and S.A. Boukabara, The microwave radiometer aboard ERS-1, Part 2 : Validation of the geophysical products, *IEEE Trans. Geosci. Remote Sensing*, 34, 291-303, 1996.

Eymard L., S. English, P. Sobieski, D. Lemaire and E. Obligis, Ocean surface emissivity modelling, COST Action 712, C. Mätzler - UE COST and Univ. Bern, Brussels, Bern, pp. 129-148, 2000.

Garand, L., D. S. Turner, M. Larocque, J. Bates, S. Boukabara, P. Brunel, F. Chevalier, G. Deblonde, R. Engelen, M. Hollingshead, D. Jackson, G. Jedlovec, J. Joiner, T. Kleespies, D. S. McKague, L. McMillin, J.-L. Moncet, J. R. Pardo, P. J. Rayner, E. Salathe, R. Saunders, N. A. Scott, P. Van Delst, and H. Woolf. 2001, Radiance and Jacobian intercomparison of radiative transfer models applied to HIRS and AMSU channels. *J. Geophys. Res.*, 106, 24017-24031.

CLS -	Final Report on activities performed in 2002-2004 on the ERS2/MWR survey	Page : 46 Date : 2004-12-10
Source ref : CLS-DOS-NT-04-255	Nomenclature : -	Issue : 1 rev. 0

Janssen M. A., C. S.Ruf and S. J.Keihm, TOPEX/Poseidon Microwave Radiometer (TMR) :
II. Antenna Pattern Correction and Brightness Temperature Algorithm, *IEEE Trans. Geosci. And Remote Sensing*, 33, 138-146, 1995.

Karbou, F., L. Eymard, C. Prigent et J. Pardo, Microwave land emissivity assessment using AMSU-A and AMSU-B measurements, *IGARSS03*, July 2003, Toulouse, France.

Karbou, F., C. Prigent, L. Eymard, and J. Pardo, 2004, Microwave land emissivity calculations using AMSU-A and AMSU-B measurements, *IEEE Trans on Geoscience and Remote sensing*, TGRS-00185-2004, to be published

Keihm S. J., V. Zlotnicki and C. S. Ruf, TOPEX Microwave Radiometer performance evaluation, 1992-1998, *IEEE Trans. Geosci. Rem. Sens.*, 38(3), 2000.

Keihm S., M. Janssen and C. Ruf, TOPEX/POSEIDON Microwave Radiometer (TMR) : III. Wet tropospheric correction and pre-launch error budget, *IEEE Trans. Geosci. Rem. Sens.*, 33, 147-161, 1995.

Mu T., AMSU-A antenna pattern corrections, *IEEE Transactions of Geosciences and Remote Sensing*, Vol. 37, NO 1, January 1999.

Obligis E., N. Tran and L. Eymard, ERS-2 drift evaluation and correction, Tech. Rep., CLS/DOS/NT/03.688, 2003.

Obligis E., Tran N. and L. Eymard, An assessment of Jason-1 microwave radiometer measurements and products, *Marine Geodesy*, 27, 255-277, 2004.

Pardo J. R., C. Prigent, S. English and P. Brunel, Comparison of Direct Radiative Transfer Models in the 60 GHz O2 band with SSM/T-1 and MSU observations, 8th TOVS conference, Auckland (New Zealand), 1995.

Pardo, J.P., J. Cernicharo and E. Serabyn, 2001, Atmospheric Transmission at Microwave (ATM): an improved model for millimetre/submillimeter applications, *IEEE Trans. Ant and Prop*, vol. 49, NO. 12, pp. 1683-1694.

Prigent, C., J.-P. Wigneron, W.B. Rossow, and J.R. Pardo-Carrion, Frequency and angular variations of land surface microwave emissivities: Can we estimate SSM/T and AMSU emissivities from SSM/I emissivities?. *IEEE Trans. Geosci. Remote Sensing* 38, 2373-

CLS -	Final Report on activities performed in 2002-2004 on the ERS2/MWR survey	Page : 47 Date : 2004-12-10
Source ref : CLS-DOS-NT-04-255	Nomenclature : -	Issue : 1 rev. 0

2386, 2000.

Prigent, C., W.B. Rossow, and E. Matthews, 1997, Microwave land surface emissivities estimated from SSM/I observations, *J. Geophys. Res.*, vol. 102, pp. 21 867-21 890.

Rossow, W. B. and R. A. Schiffer, 1991, ISCCP cloud data products, *Bull. Am. Meteor. Soc.*, 72, pp. 2-20.

Ruf C., S. Brown, S. Keihm and A. Kitiyakara, JASON Microwave Radiometer : On Orbit Calibration, Validation and Performance, Jason-1/TOPEX/Poseidon Science Working Team Meeting, 21-23 October 2002, New Orleans, 2002.

Ruf, C., S. Keihm, B. Subramanya and M. Janssen, TOPEX/POSEIDON microwave radiometer performance and in-flight calibration, *J. Geophys. Res.*, 99, 24, 915-24, 926, 1994.

Ruf C.S., S.J. Keihm and M.A. Janssen, TOPEX/Poseidon Microwave Radiometer (TMR) : I. Instrument description and Antenna Temperature Calibration, *IEEE Trans. Geosci. and Remote Sensing*, 33, 1, 125-137, 1995.

Ruf, C.S., Detection of calibration drifts in spaceborne microwave radiometers using a vicarious cold reference, *IEEE Trans. Geosci. and Remote Sensing*, 38, 44-52, 2000.

Scharroo R., J. Lillibrige and W. Smith, Cross-calibration and Long-term Monitoring of the Microwave Radiometers of ERS, TOPEX, GFO, Jason and Envisat, submitted to Marine Geodesy, 2003.

Simmons, A. J., and J.K. Gibson, the European Centre for Medium-Range Weather Forecasts: The ERA-40 Project Plan, 2000.

Skou, N., Microwave radiometer systems: design and analysis Artech House, ISBN 0-89006-368-0, 1989.

Stum, J., 1998. Comparison of the brightness temperatures and water vapor path delays measured by the TOPEX, ERS-1 and ERS-2 microwave radiometers. *Journal of Atmospheric and Oceanic Technology*, 15, 987-994.

Stum J., F. Mertz and J. Dorandeu, Long-term monitoring of the OPR altimeter data quality, Infremer contract n°00/2.210052, 2001.

Torinesi, O., M. Fily and C. Genthon, Variability and Trends of the Summer Melt Period of Antarctic Ice Margins since 1980 from Microwave Sensors. *J. Climate*, 16, (7) 1047-1060, 2003.

Tran N., Obligis E., and L. Eymard : In-flight Calibration/Validation of ENVISAT microwave radiometer, Proceedings IGARSS, Toulouse, July 2003.

Ulaby, F.T., R.K. Moore, and A.K. Fung, Microwave remote sensing: fundamentals and radiometry, volume 1. Artech House, 1981.

<p style="text-align: center;">CLS</p> <p style="text-align: center;">-</p>	<p style="text-align: center;">Final Report on activities performed in 2002-2004 on the ERS2/MWR survey</p>	<p>Page : 48</p> <p>Date : 2004-12-10</p>
<p>Source ref : CLS-DOS-NT-04-255</p>	<p>Nomenclature : -</p>	<p>Issue : 1 rev. 0</p>

Weng, F., L. Zhao, R. Ferraro, G. Poe, X. Li, N. Grody, 2003: Advanced Microwave Sounding Unit Cloud and Precipitation Algorithms. Radio Sci., 38, 8,086-8,096.

CLS -	Final Report on activities performed in 2002-2004 on the ERS2/MWR survey	Page : 49 Date : 2004-12-10
Source ref : CLS-DOS-NT-04-255	Nomenclature : -	Issue : 1 rev. 0

Tables

Table 1 : main characteristics of the ERS / ENVISAT and TOPEX/Jason altimeter missions.

Table 2 : trends obtained with the two methods for the TMR and EMWR radiometers. For the TMR the trends are estimated for a 7 years period, and for the EMWR for a 6 years period. The first column corresponds to the “cold ocean” method presented in section 3.1, the second one to selection of “cold” data on cross over locations (EMWR / TMR), the third refers to the study of Scharroo et al (2004), and the fourth to the study of TMR drift by Ruf et al, 2000.

Table 3 : location of target areas for long term survey of the ERS2 radiometer and the TMR (except for the Antarctic plateau).

Table 4 : Long term trends of the EMWR TBs over stable continental areas for a six years period. The last column is the relative trend over the same duration for all areas.

Table 5 : Long term trends of the TMR TBs over stable continental areas for all the period.

Table 6 : intercomparison results between TMR and EMWR brightness temperatures over the 3 selected areas.

Table 7 : AMSU-A brightness temperatures over the Amazon Forest area. The statistical indicators were computed with the nighttime and daytime passes respectively for the four seasons.

Table 8 : Means and standard deviations of the brightness temperatures over the frequency range from 18.0 to 37.0 GHz at nadir and for nighttime hours.

Table 9 : Mean emissivity over Amazon forest for January, 2000 for AMSU-A, TMR and SSMI channels in the 18 – 37 GHz range. The first number gives the mean, the second one the standard deviation. Note that the SSM/I emissivity at 22 GHz is not reported, because the calculation of the equivalent AMSU emissivity requires two polarizations.

CLS -	Final Report on activities performed in 2002-2004 on the ERS2/MWR survey	Page : 50 Date : 2004-12-10
Source ref : CLS-DOS-NT-04-255	Nomenclature : -	Issue : 1 rev. 0

Figure captions

Figure 1: Long term monitoring of the coldest TBs over the ocean for TMR and EMWR. Dates (in days) are referenced to 1st January 1991. TBs are in K. Channels are labeled by their frequency (18, 21 and 37 GHz). a) TMR. The linear fit over the first 7 years is superimposed. b) EMWR. The linear fit over the last 6 years is superimposed.

Figure 2 : TMR and EMWR brightness temperatures as a function of the CNES julian day. Selected pixels are cross-over points with ERS2 for which TMR brightness temperatures at 21 GHz are lower than 134 K. a) TMR; b) EMWR

Figure 3 : Drift of the ERS2 and TOPEX wet tropospheric correction, using cross-over points between the two missions and selecting the coldest TMR 21 GHz brightness temperatures over ocean.

Figure 4: Time series of EMWR 23.8 GHz channel over the five selected continental areas. a) Coldest Antarctic Plateau (Antarctic-1); b) Antarctic-2 area; c) Sahara desert (ascending orbits); d) Amazon forest (ascending orbits); e) Greenland. In the latter case, the original time series is in red, and the selected data after removing the melting ice data are superimposed in green,

Figure5 : Mean diurnal cycle of TMR brightness temperatures over the Amazon forest

Figure 6: Map of vegetation classes, from Dickinson, 1986, which was used to select the deep forest area (in blue)

Figure 7: Monthly mean maps (over January, 2000), of the AMSU-A 23.8 GHz (top), EMWR 23.8 GHz (middle) and TMR 21 GHz (bottom) channels. Left: mean emissivity maps; right: emissivity standard deviation. Maps are displayed on a regular grid of mesh 0.5deg. in longitude and latitude. Meshes for which the mean emissivity is lower than 0.9 and the standard deviation is greater than 0.03 were removed.

Figure 8: mean diurnal cycle of the retrieved emissivities at 210/023.8 GHz, over the month for the entire forest area. Black: AMSU-A; blue: TMR; red: EMWR.

CLS -	Final Report on activities performed in 2002-2004 on the ERS2/MWR survey	Page : 51 Date : 2004-12-10
Source ref : CLS-DOS-NT-04-255	Nomenclature : -	Issue : 1 rev. 0

Tables

MISSION	ERS1	TOPEX / TMR	ERS2 / EMWR	JASON1/J MR	ENVISAT	NOAA/ AMSU-A	DMSP/ SSM/I
Life in space	1991-1996	1992-	1995-	2001-	2002-	2000-	1987 -
Altimeter Frequencies (GHz)	13.8	Topex : 13.6 5.3 Poseidon : 13.6	13.8	13.575 5.3	13.575 3.2	—	—
Radiometer Channels (GHz)	23.8 36.5	18 21 37	23.8 36.5	18.7 23.8 34	23.8 36.5	23.8 31.4 50 (and oxygen absorption band) 89	18.7 22 37 89 (H and V except 22)
other information on measurements	Incidence angle +2.5 (23.8) and -1.5 (36.5) Footprint 20/22 km at 3dB	Nadir pointing - 21 and 37 GHz measurements interpolated on the 18 GHz footprint	Isame as ERS1	Similar to TOPEX/T MR	Same as ERS1	Transverse scanning (7sec period) Footprint size 40 km at 23.8, ??? at nadir	Comical scanning Footprint size 60 km at 18.7 GHz, 40 at 22, 25 km at 37 and 12.5 at 89 GHz
Orbit	Sun-synch.		Sun-synch.		Sun-synch.	Sun-synch.	Sun-synch.
Inclination	98°	62°	98°	62°	98°	7:00 descending	7:00 descending
Cycle	35 days	10 days	35 days	10 days	35 days	7:00 descending	7:00 descending
Node	10:30 desc.		10:30 desc.		10:30 desc.		

Table 1 : main characteristics of the ERS / ENVISAT and TOPEX/Jason altimeter missions and the on board radiometers. For comparison, SSMI and AMSU-A major characteristics are also given.

CLS -	Final Report on activities performed in 2002-2004 on the ERS2/MWR survey	Page : 52 Date : 2004-12-10
Source ref : CLS-DOS-NT-04-255	Nomenclature : -	Issue : 1 rev. 0

Instrument	Channels (GHz)	Drift Cold Ocean (K/year)	Drift Cross-overs (K/year)	Drift Sharroo et al (K/year)	Drift Ruf et al (K/year)
TMR	18.0	0.21	0.1±0.06	0.21	0.26
	21.0	0.02	-0.02±0.04	0.03	-
	37.0	0.04	0.08±0.08	0.02	-
EMWR	23.8	-0.27	-0.2±0.1	-0.1	-
	36.5	0.03	0.05±0.1	-	-

Table 2 : trends values for the TMR and EMWR radiometers. For the TMR the trends are estimated for a 7 years period, and for the EMWR for a 6 years period. The first column corresponds to the “cold ocean” method presented in section 3.1, the second one to selection of “cold” data on cross over locations (EMWR / TMR), the third refers to the study of Scharroo et al (2004), and the fourth to the study of TMR drift by Ruf et al, 2000.

Area	South latitude	North latitude	West longitude	East longitude
Antarctic plateau (1)	-81.3	-81.0	114.0 E	116.0 E
Antarctic plateau (2)	-81.5	-81.2	135.5 E	137.5 E
Greenland plateau	65.0	66.0	47.0 W	43.0 W
Sahara desert	18.9	19.4	5.7W	4.8 W
Amazon forest	- 5.5	-4.5	67.0 W	64.5 W

Table 3 : location of target areas for long term survey of the ERS2 radiometer and the TMR (except for the Antarctic plateau).

CLS -	Final Report on activities performed in 2002-2004 on the ERS2/MWR survey	Page : 53 Date : 2004-12-10
Source ref : CLS-DOS-NT-04-255	Nomenclature : -	Issue : 1 rev. 0

AREA	23.8 GHz (ch 1) K/year	36.5 GHz (ch 2) K/year	ch2 – ch 1 trends K/year
Antarctic 1 (coldest)	0.003	0,213	0.180
Antarctic 2	-0,147	-0,060	0.087
South Greenland	0.865	0.880	0.015
Sahara night	0.097	-0.053	-0.150
Sahara day	0.202	-0.036	-0.239
Amazon forest night	0.029	-0.082	-0.111
Amazon forest day	-0.107	-0.281	-0.173

Table 4 : Long term trends of the EMWR TBs over stable continental areas for a six years period (first year not processed). The last column is the relative trend over the same duration for all areas.

Area	18 GHz	21 GHz	37 GHz
Greenland	0.302	0.256	0.275
Sahara night	0,244	0.230	0.267
Sahara day	0.197	0.163	0.190
Amazon forest night	0.050	0.050	0.093
Amazon forest day	0.060	0.063	0.193

Area	mean differences between channel trend (9 years) K/year	
	21-18 GHz	37 -21 GHz
Greenland	-0,046	0.019
Sahara night	-0.014	0.037
Sahara day	-0.033	0.027
Amazon forest night	0.001	0.043
Amazon forest day	-0.003	0.130

Table 5 : Long term trends of the TMR TBs over stable continental areas for a nine year period (K/year).

CLS -	Final Report on activities performed in 2002-2004 on the ERS2/MWR survey	Page : 54 Date : 2004-12-10
Source ref : CLS-DOS-NT-04-255	Nomenclature : -	Issue : 1 rev. 0

Area	TMR mean Tbs over 9 years (K)			EMWR over 7 years (K)	
	18 GHz	21 GHz	37 GHz	23.8 GHz	36.5 GHz
Greenland	160.98	166.22	180.32	167.55	182.56
Sahara night	276.25	275.12	276.19	281.41	288.64
Sahara day	276.71	275.91	277.93	283.33	291.33
Amazon forest night	279.55	278.91	278.74	285.46	291.49
Amazon forest day	283.72	282.42	282.76	289.13	295.54

Table 6 : intercomparison between TMR and EMWR mean brightness temperatures over the 3 selected areas for EMWR overpass times.

CLS -	Final Report on activities performed in 2002-2004 on the ERS2/MWR survey	Page : 55 Date : 2004-12-10
Source ref : CLS-DOS-NT-04-255	Nomenclature : -	Issue : 1 rev. 0

Nighttime	TB, Mean +/- Standard Deviation, K				Number of points
	23.8 GHz		31.4 GHz		
Winter	286.0	1.1	283.1	1.5	185
Spring	285.5	1.0	282.2	1.4	163
Summer	285.5	0.9	282.3	1.1	155
Autumn	286.3	0.8	283.3	1.0	138
All year	285.8	1.0	282.7	1.4	641

Daytime	TB, Mean +/- Standard Deviation, K				N
	23.8 GHz		31.4 GHz		
Winter	290.9	2.1	288.5	2.3	107
Spring	290.5	2.0	288.1	2.2	106
Summer	290.3	1.5	287.9	1.7	111
Autumn	291.8	1.9	289.5	2.0	94
All year	290.9	1.9	288.5	2.1	418

Table 7 : AMSU-A brightness temperatures over the Amazon Forest area. The statistical indicators were computed with the nighttime and daytime passes respectively for the four seasons.

CLS -	Final Report on activities performed in 2002-2004 on the ERS2/MWR survey	Page : 56 Date : 2004-12-10
Source ref : CLS-DOS-NT-04-255	Nomenclature : -	Issue : 1 rev. 0

Mean TB (K) and standard deviation in parenthesis (K)									
Freq	18.0	18.7	21.0	23.8	31.4	34.0	36.5	37.0	#
AMSU-A	-	-	-	285.8 (1.0)	282.7 (1.4)	-	-	-	641
TMR	278.6 (1.4)	-	278.1 (1.3)	-	-	-	-	277.6 (2.8)	2160
EMWR	-	-	-	285.7 (1.5)	-	-	291.9 (2.2)	-	3937
SSM/I	-	284.2 (1.3)	-	283.4 (1.6)	-	-	-	280.5 (2.4)	14564

Table 8 : Means and standard deviations of the brightness temperatures over the frequency range from 18.0 to 37.0 GHz at nadir and for nighttime hours.

Freq (GHz)	18.7 and 19	21.0	23.8	31.4	36.5 and 37.0
AMSU-A		-	0.960 (0.020)	0.947 (0.019)	-
TMR	0.851 (0.023)	0.921 (0.022)	-	-	0.927 (0.022)
EMWR			0.962 (0.018)		0.974 (0.022)
SSM/I	0.952	-	-	-	0.933

Table 9 : Mean emissivity over Amazon forest for January, 2000 for AMSU-A, TMR, EMWR and SSMI channels in the 18 – 37 GHz range. The first number gives the mean, the second one the standard deviation (in parentheses. Note that the SSM/I emissivity at 22 GHz is not reported, because the calculation of the equivalent AMSU-A emissivity requires two polarizations.

CLS -	Final Report on activities performed in 2002-2004 on the ERS2/MWR survey	Page : 57 Date : 2004-12-10
Source ref : CLS-DOS-NT-04-255	Nomenclature : -	Issue : 1 rev. 0

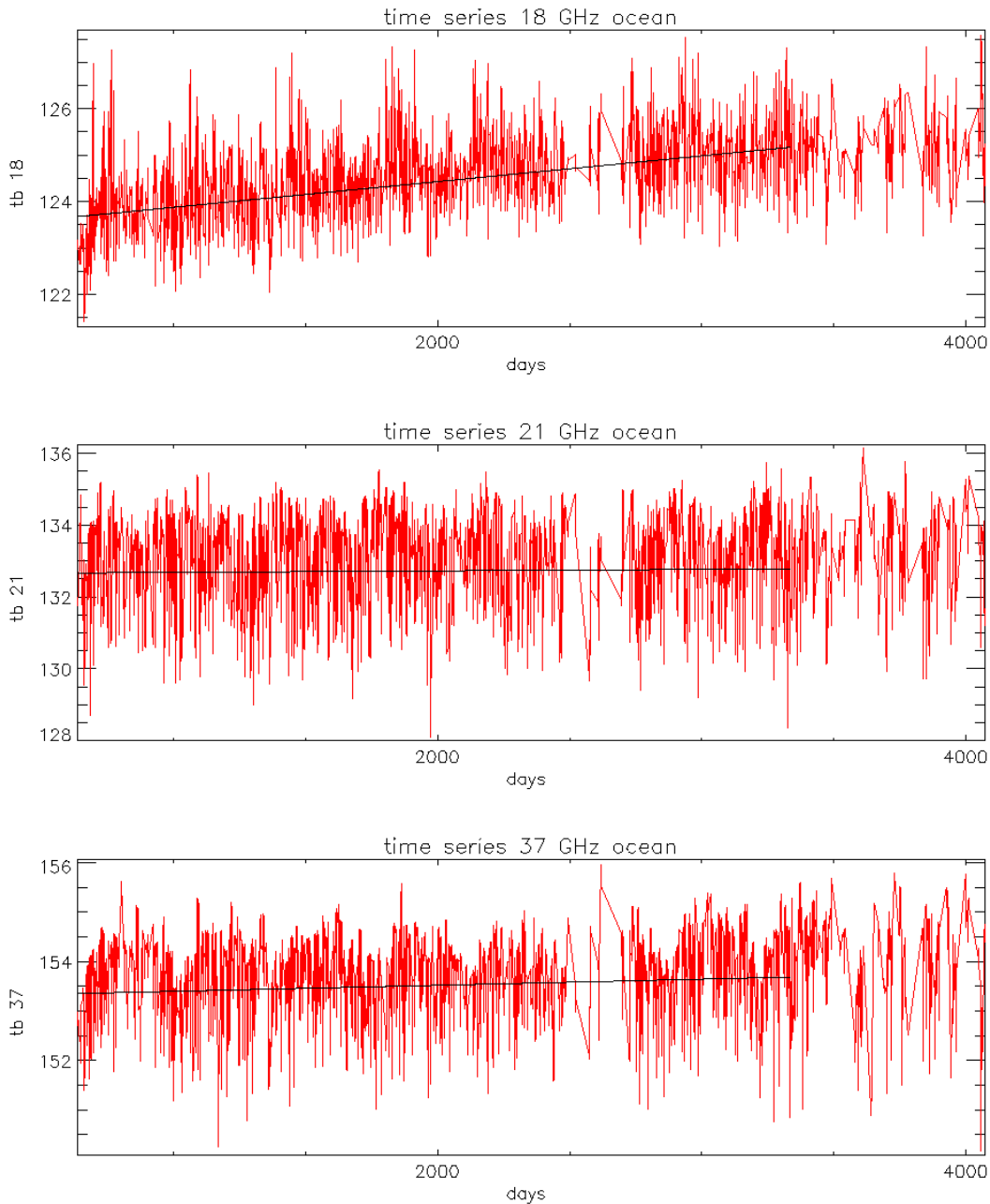


Figure 1-a : Long term monitoring of the coldest TBs over the ocean for TMR (August 1993 – December 2001). Dates (in days) are referenced to 1st January 1991. TBs are in K. Channels are labeled by their frequency (18, 21 and 37 GHz). The linear fit over 7 years is superimposed.

CLS -	Final Report on activities performed in 2002-2004 on the ERS2/MWR survey	Page : 58 Date : 2004-12-10
Source ref : CLS-DOS-NT-04-255	Nomenclature : -	Issue : 1 rev. 0

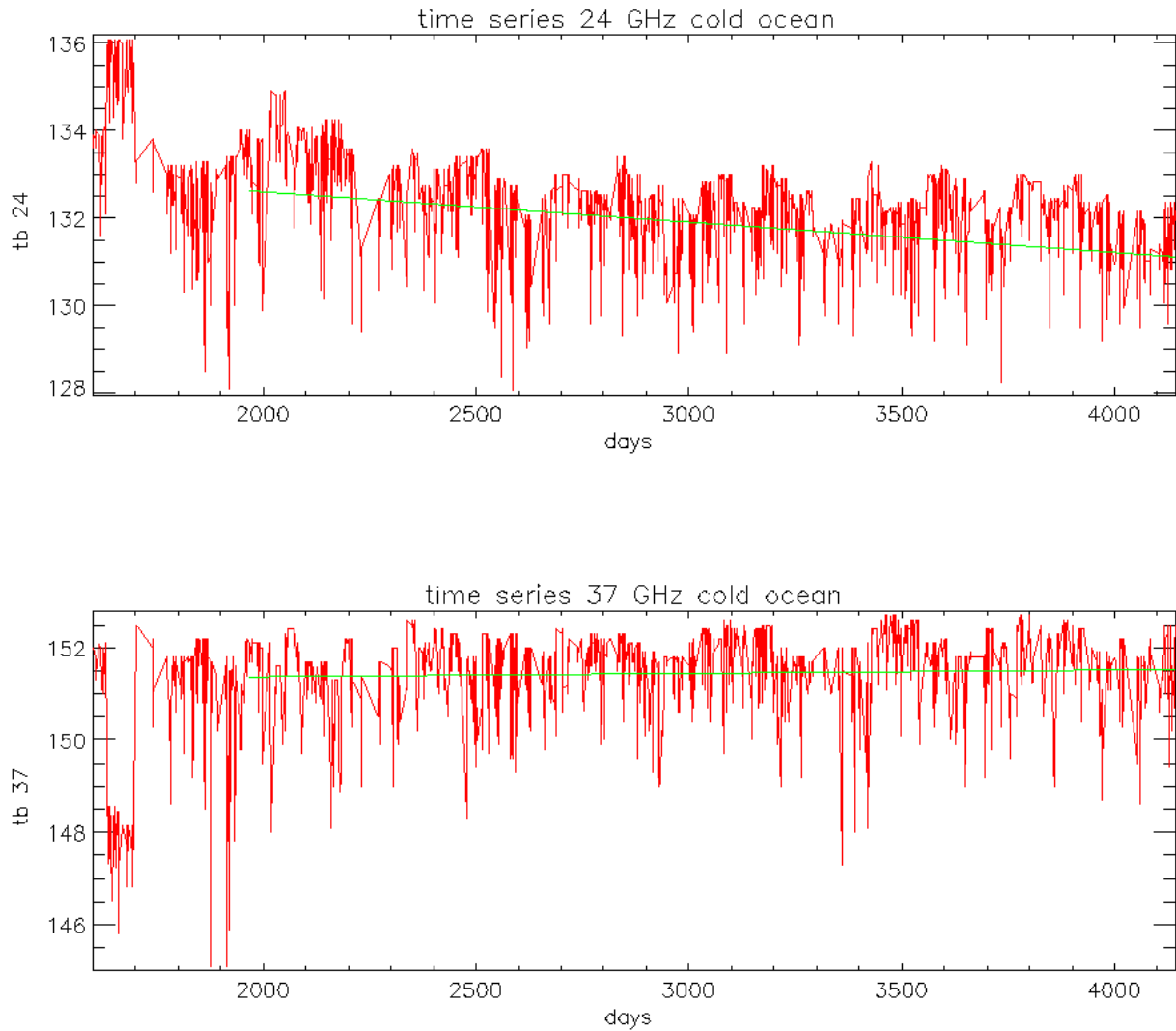


Figure 1-b : Long term monitoring of the coldest TBs over the oceans for EMR. Dates (in days) are referenced to 1st January 1991 (May 1995 – January 2002). TBs are in K. Channels are labeled by their frequency (24 for 23.8 GHz and 37 for 36.5 GHz). The linear fit over the last 6 years is superimposed.

CLS -	Final Report on activities performed in 2002-2004 on the ERS2/MWR survey	Page : 59 Date : 2004-12-10
Source ref : CLS-DOS-NT-04-255	Nomenclature : -	Issue : 1 rev. 0

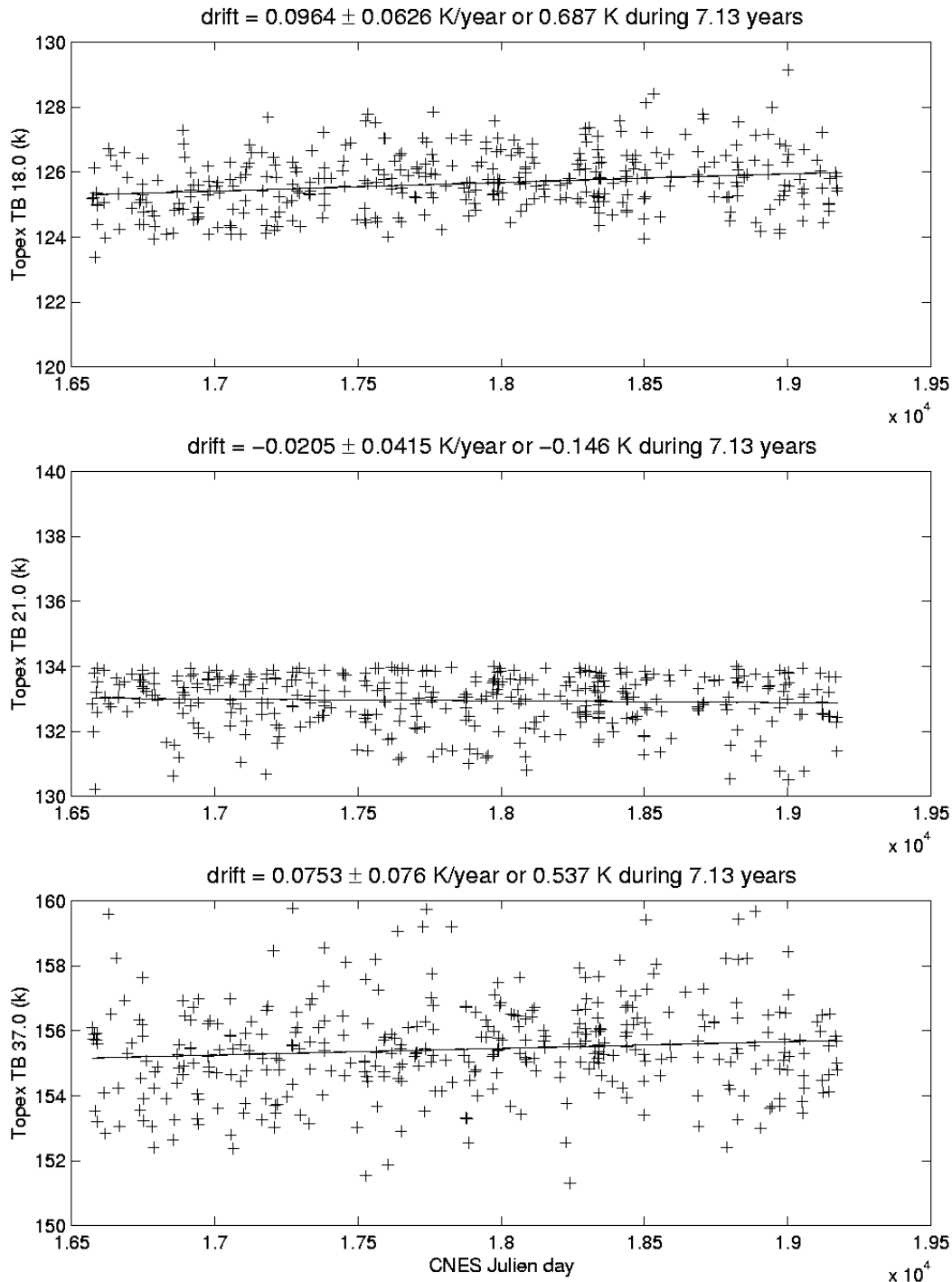


Figure 2-a : TMR brightness temperatures as a function of the CNES julian day (January 1995 – July 2002). Selected pixels are cross-over points with ERS2 for which TMR brightness temperatures at 21 GHz are lower than 134 K.

CLS -	Final Report on activities performed in 2002-2004 on the ERS2/MWR survey	Page : 60 Date : 2004-12-10
	Source ref : CLS-DOS-NT-04-255	Nomenclature : -

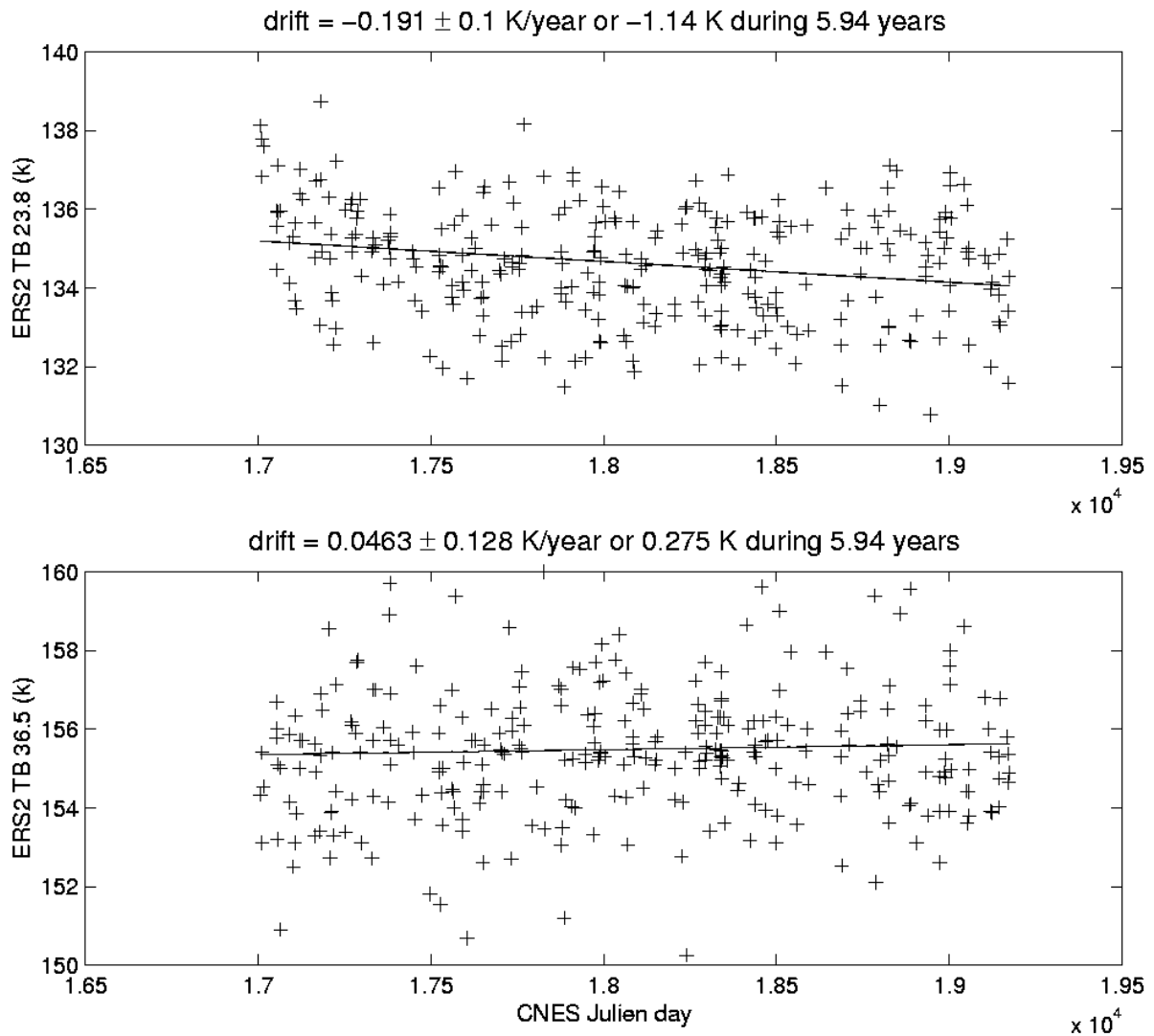


Figure 2-b : EMWR brightness temperatures as a function of the CNES julian day (July 1996 – July 2002). Selected pixels are cross-over points with TOPEX for which TMR brightness temperatures at 21 GHz are lower than 134 K.

CLS -	Final Report on activities performed in 2002-2004 on the ERS2/MWR survey	Page : 61 Date : 2004-12-10
Source ref : CLS-DOS-NT-04-255	Nomenclature : -	Issue : 1 rev. 0

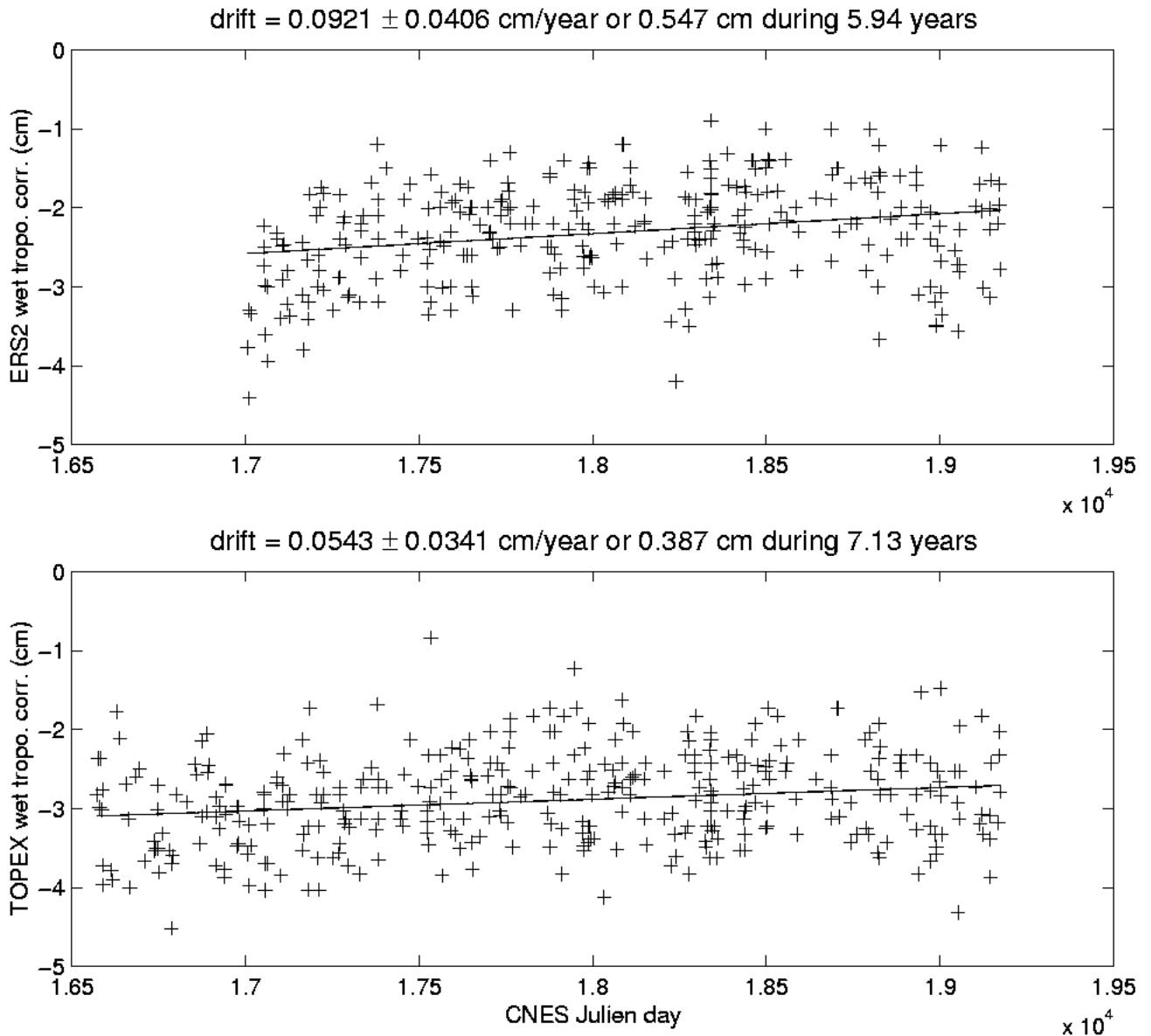
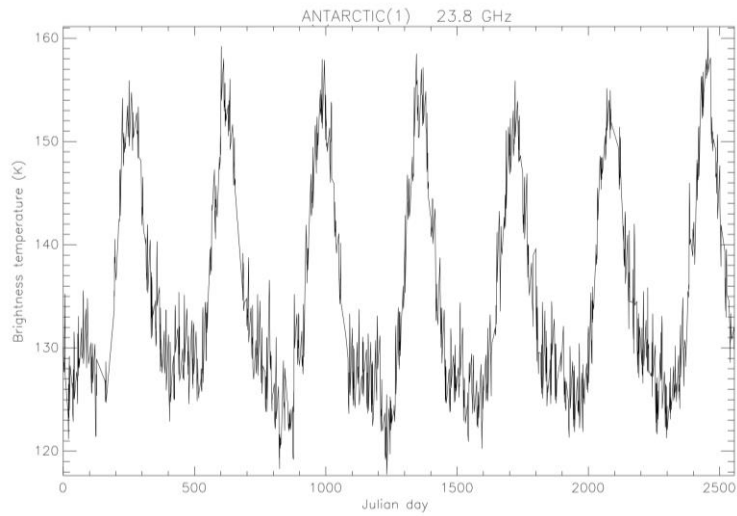
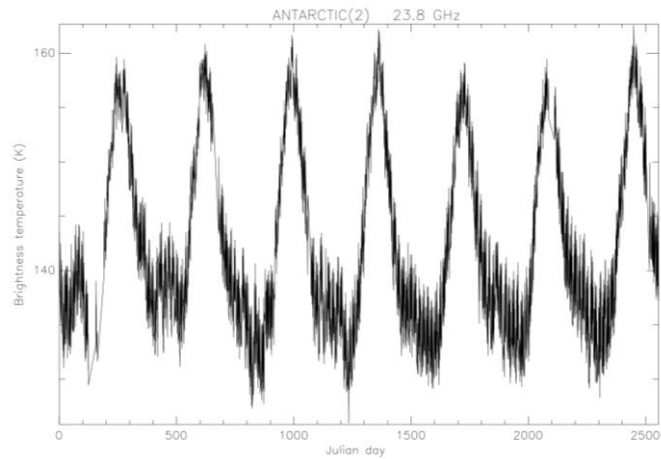


Figure 3 : Drift of the ERS2 and TOPEX wet tropospheric correction, using cross-over points between the two missions and selecting the coldest TMR 21 GHz brightness temperatures over ocean.

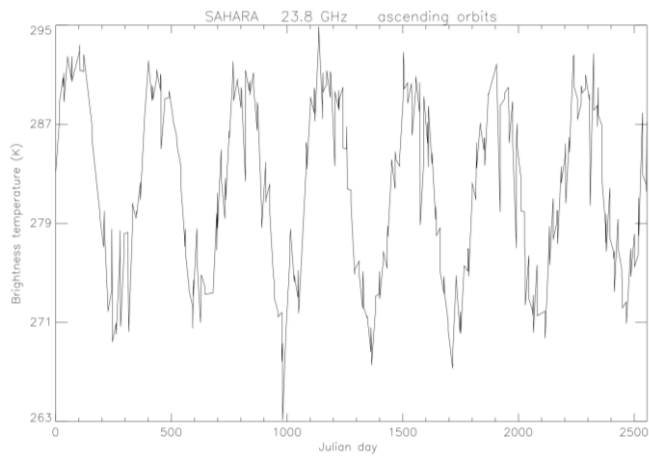
<p>CLS -</p>	<p>Final Report on activities performed in 2002-2004 on the ERS2/MWR survey</p>	<p>Page : 62 Date : 2004-12-10</p>
<p>Source ref : CLS-DOS-NT-04-255</p>	<p>Nomenclature : -</p>	<p>Issue : 1 rev. 0</p>



a

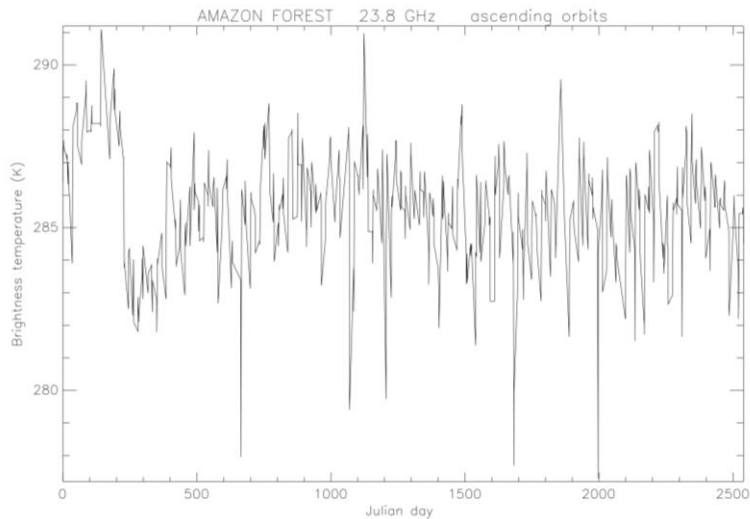


b

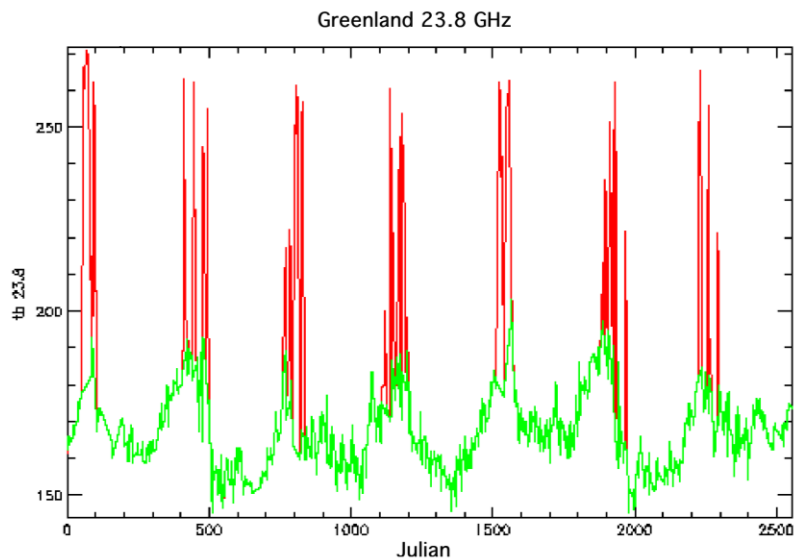


c

CLS -	Final Report on activities performed in 2002-2004 on the ERS2/MWR survey	Page : 63 Date : 2004-12-10
Source ref : CLS-DOS-NT-04-255	Nomenclature : -	Issue : 1 rev. 0



d



e

Figure 4: Time series of EMWR 23.8 GHz channel over the five selected continental areas. a) Coldest Antarctic Plateau (Antarctic-1); b) Antarctic-2 area; c) Sahara desert (ascending orbits); d) Amazon forest (ascending orbits); e) Greenland. In the latter case, the original time series is in red, and the selected data after removing the melting ice data are superimposed in green.

CLS -	Final Report on activities performed in 2002-2004 on the ERS2/MWR survey	Page : 64 Date : 2004-12-10
Source ref : CLS-DOS-NT-04-255	Nomenclature : -	Issue : 1 rev. 0

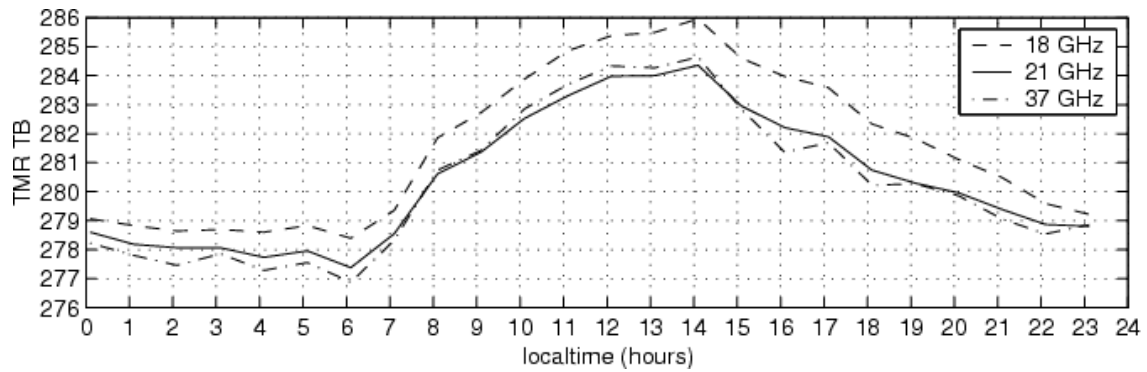


Figure5 : Mean diurnal cycle of Topex brightness temperatures over the Amazon forest

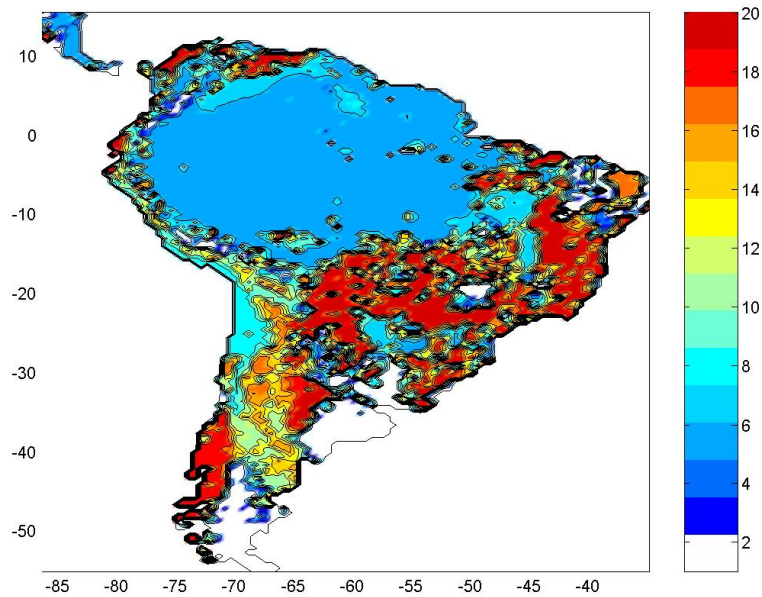


Figure 6: Map of vegetation classes, from Dickinson, 1986, which was used to select the deep forest area (in blue)

CLS -	Final Report on activities performed in 2002-2004 on the ERS2/MWR survey	Page : 65 Date : 2004-12-10
Source ref : CLS-DOS-NT-04-255	Nomenclature : -	Issue : 1 rev. 0

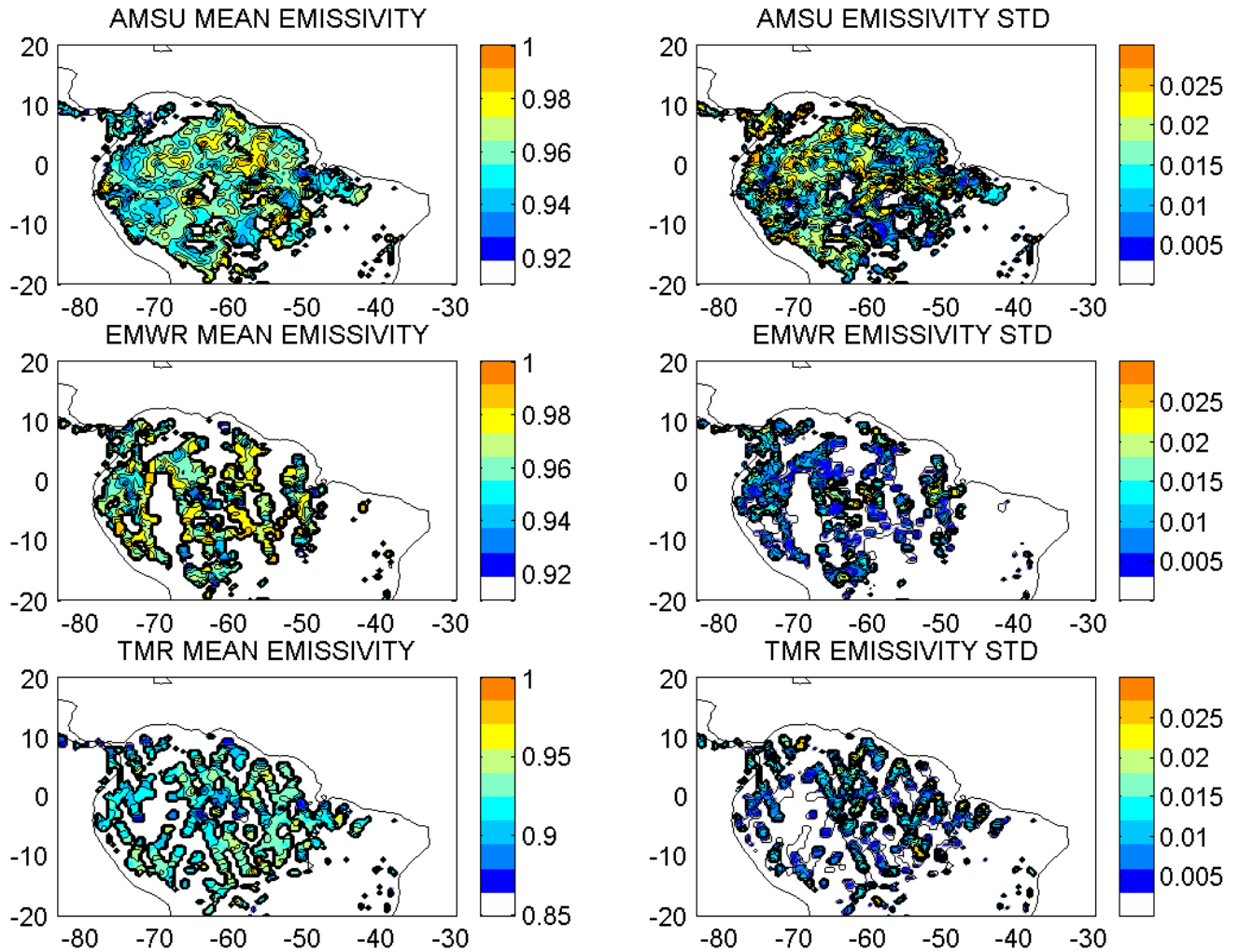


Figure 7: Monthly mean maps (over January, 2000), of the AMSU-A 23.8 GHz (top), EMWR 23.8 GHz (middle) and TMR 21 GHz (bottom) channels. Left: mean emissivity maps; right: emissivity standard deviation. Maps are displayed on a regular grid of mesh 0.5deg. in longitude and latitude. Meshes for which the mean emissivity is lower than 0.9 and the standard deviation is greater than 0.03 were removed.

CLS -	Final Report on activities performed in 2002-2004 on the ERS2/MWR survey	Page : 66 Date : 2004-12-10
Source ref : CLS-DOS-NT-04-255	Nomenclature : -	Issue : 1 rev. 0

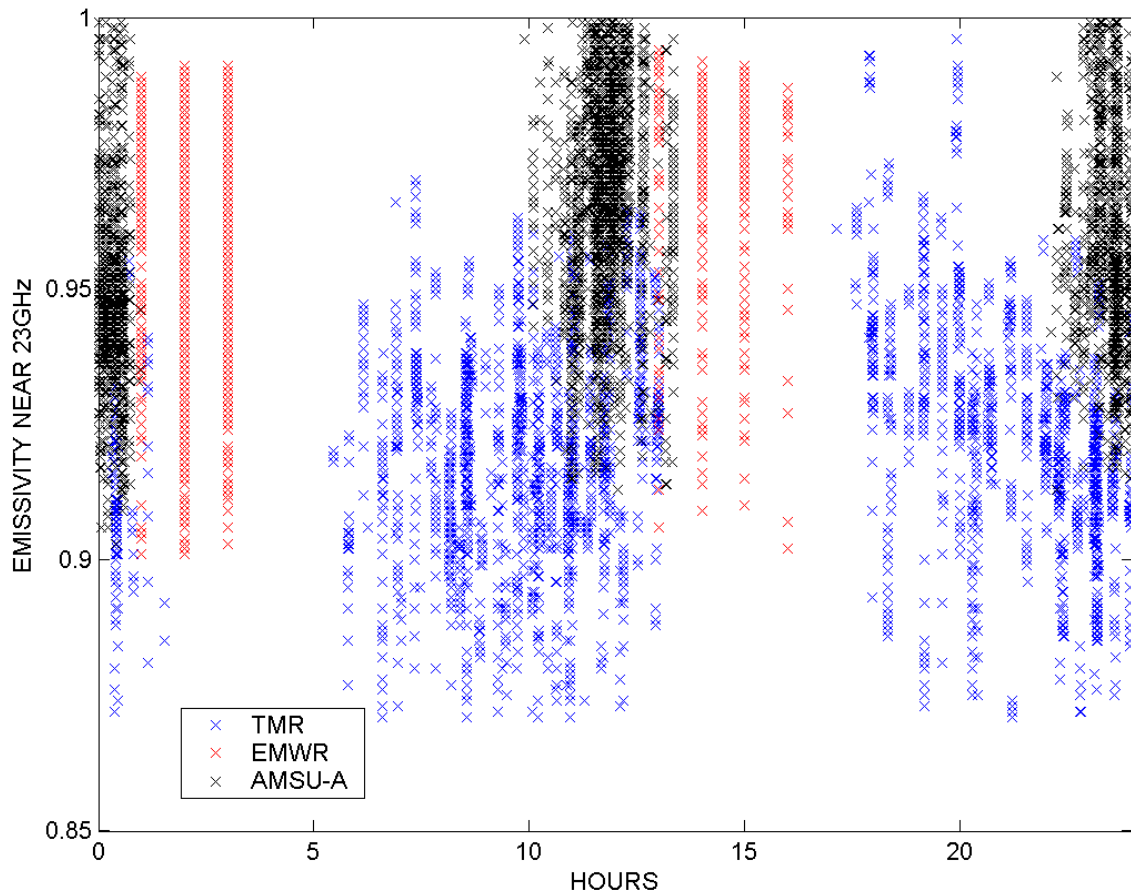


Figure 8: mean diurnal cycle of the retrieved emissivities at 210/023.8 GHz, over the month for the entire forest area. Black: AMSU-A; blue: TMR; red: EMWR.

CLS -	Final Report on activities performed in 2002-2004 on the ERS2/MWR survey	Page : 67 Date : 2004-12-10
Source ref : CLS-DOS-NT-04-255	Nomenclature : -	Issue : 1 rev. 0

9. ANNEX 2

9.1. INTRODUCTION

Two corrections for the 23.8 GHz brightness temperatures are presently available (Eymard et al, 2003; Scharroo et al, 2004). They took into account both the gain loss on 16 June 1996 and an instrumental drift that occurred afterwards. The aim of this analysis is to compare the two corrective models and assess which one is more accurate and the most suitable to be recommended to ERS-2 users.

9.2. PRESENTATION OF THE TWO CORRECTIONS

9.2.1. Eymard et al's model

This model was developed, based on the following conditions: (1) no correction for cold TB (132 K) measured on the 26 June 1996 (1.18 year) and a correction of +1.6 K for cold TB (132 K) measured on the 30 September 2002 (date of the study performed by Eymard et al.); (2) no correction for hot TB (300 K) measured on the 26 June 1996 and no correction for hot TB (300 K) measured the 30 September 2002; (3) due to the linear form of the calibration model, the correction is a linear function of time and of TB value.

The resulting corrected 23.8 GHz TB is expressed as :

CLS -	Final Report on activities performed in 2002-2004 on the ERS2/MWR survey	Page : 68 Date : 2004-12-10
Source ref : CLS-DOS-NT-04-255	Nomenclature : -	Issue : 1 rev. 0

$$TB = \begin{cases} TB_{OPR} & \text{for } t \leq 1.183 \\ TB_{gaindrop} + \Delta TB & \text{for } t > 1.183 \\ \text{with } TB_{gaindrop} = 0.93 \cdot TB_{OPR} + 19.18 \\ \text{and } \Delta TB = (a1 \cdot t + a2) \cdot TB_{gaindrop} + (b1 \cdot t + b2) \\ a1 = -0.001521; a2 = 0.001795; b1 = 0.4564; b2 = -0.5386 \end{cases}$$

where t is the time in year since the launch of ERS-2 (21 April 1995).

9.2.2. Scharroo et al's model

This model was developed, based on the following conditions: (1) scale and offset of the TB after the gain loss should be adjusted so that both the coldest and mean TB are brought in line with those before the gain loss; (2) the resulting temperature of no change (314.5 K) remains constant throughout the drift; (3) a certain periode of relaxation is to be accounted for; (4) the drift stops around April 2000.

The resulting correction, to be subtracted from the 23.8 GHz TB that are provided in the ERS-2 Ocean Products (OPR), is a product of a function of brightness temperature, $f(TB)$, and a function of time, $g(t)$, as : $\Delta TB = f(TB) \cdot g(t)$ with

$$f(TB) = 1 - TB / 314.5$$

$$g(t) = \begin{cases} 0 & \text{for } t < 1.183 \\ -17.889 - 0.201 \cdot t + 0.688 / (t - 1.102) & \text{for } 1.183 \leq t < 5.0 \\ -18.717 & \text{for } t > 5.0 \end{cases}$$

Figure 1 are from Scharroo et al's paper (2004) where they outlined several shortcomings from Eymard et al's (2003) proposed correction. We recall them here to help to understand the comparison results provided below. There are four of them: (1) the instrumental drift

CLS -	Final Report on activities performed in 2002-2004 on the ERS2/MWR survey	Page : 69 Date : 2004-12-10
Source ref : CLS-DOS-NT-04-255	Nomenclature : -	Issue : 1 rev. 0

seems to ceased around April 2000; (2) although the coldest TB is well calibrated accross the gain loss event, the mean TB drops considerably more than modeled; (3) the short period of relaxation after the gain loss is not account for; and (4) the single TB that remains unchanged when applying the correction changes with time.

The two models are displayed in Figure 1. For coldest TBs, the corrections are not significantly different from each others. While the mean TB gained about 0.5 K by January 1997 with Scharroo et al's model and almost 1 K by April 2000 as pointed out in their paper. This equates to about 2 mm and 4 mm of change in the mean wet tropospheric delay, or a mean rate of more than 1 mm/year. After the drift ceased, the corrections to the mean TB converged again by the end of the global ERS-2 mission in August 2003, leading to effectively the same average correction to the wet tropospheric delay as they reported. The next section will provide another assessment and verification of the difference between the two corrections.

9.3. COMPARISON OF THE TWO CORRECTIONS

Figure 2 shows the time series of different ERS-2 mean 23.8 GHz TB values, from OPR and after application of either one of the available orrections. On the OPR data, we observe the gain drop that occured on June 1996 resulting in the decrease of the 23.8 GHz TB that stabilized at a level of ~160 K after several cycles. The bottom panel is a zoom on the corrected TB. As we can observe, between the end of 1996 and mid 2000, the two corrections are not significantly different for the mean TB. Before this period (period of transition), small differences are observed and they decrease with time. From mid 2000, differences increase and are up to 0.8 K by mid 2003 due to the fact that the instrumental drift has ceased. This was taken into account into Scharroo et al's model while in the Eymard et al's one the correction of the drift remains with the same slope leading to an overcompensation that increases with time. The flatness of the corrected TB with time will be evaluated in Figure 4 and Table 1. Note the lower standard deviation of the cycle TB averages in the case of the application of Scharroo et al's correction.

CLS -	Final Report on activities performed in 2002-2004 on the ERS2/MWR survey	Page : 70 Date : 2004-12-10
Source ref : CLS-DOS-NT-04-255	Nomenclature : -	Issue : 1 rev. 0

The standard deviation of the different TB computed over the different cycles is displayed in Figure 3. Both corrections tend to decrease similarly the range of variation of the TB when comparing with the estimates from OPR data. This feature is explained by the fact that due to the inhomogeneous impact of the gain drop on the TB values, i.e. the cold TB decreased much more than the hot TB, leading to an artificial increase of the range of variation of TB. Correcting the OPR TB for the gain drop and subsequent drift leads then to obtain a range of variation of the TB closer to the one observed on OPR TB before the incident.

To compare more precisely the two corrections from cycle 11 (after the gain drop) to 85 (before the failure on the tape recorder), we compute the differences between them and results are shown on Figure 4. Before analyzing this plot, note that it was computed as described next. We characterize ERS-2 OPR 23.8 GHz TB variations in time and values through a set of curves displayed in Figure 5. We compute statistical indicators on the OPR TB, mean and standard deviation, for each cycle. From them we plotted different time series defined by the cycle mean plus or minus n times the standard deviation (n goes from 0 to 2 by step of 0.2). The big solid line in the middle of the set of curves in Figure 5 represents the time series of the mean and the red curve, the mean minus 2 times the standard deviation. Then we applied on these plotted TB values both correction models and the resulting plots are provided in Figure 6. Note the difference impact on OPR TB values of the gain drop; it is larger for the cold TB than for the hot ones. After correcting the TB, the values are brought in line with those before the gain loss in both cases.

To evaluate the flatness on the corrected TB, we fitted the different curves (displayed in Figure 6) between cycles 11 to 85 by linear regression lines. The slopes of the fit and the standard deviation of the residuals are provided in Table 1 for the two sets of corrected TB. Slopes of the linear fit are always smaller when computed on Scharroo et al's corrected TB.

CLS -	Final Report on activities performed in 2002-2004 on the ERS2/MWR survey	Page : 71 Date : 2004-12-10
Source ref : CLS-DOS-NT-04-255	Nomenclature : -	Issue : 1 rev. 0

The standard deviations of the residuals are also smaller except for cases marked in light green in Table 1. So Scharroo et al's corrective model provides flatter time series of TB.

Note also that since Scharroo et al's corrective model took into account the transition period that characterizes the gain drop, the corrected TB time series are flatter after cycle 11 than the curves obtained after applying Eymard et al's model where small peaks can be observed.

This peak feature is well defined in Figure 4 where we show the differences between the two corrected TB. Other remarks are that between cycles 20 and ~55, the curves look pretty flat with time indicating that the two corrections are very similar. Afterwards the drift ceased for Scharroo et al's model while it continues for Eymard et al's one. Correction for cold TB is close to 0.1 K (cycle 30) and reaches ~1 K by cycle 82. For the mean TB, the difference between the two corrections goes from -0.5 K (cycle 30) to +0.2 K (cycle 82). For the hot TB, that goes from -1.3 K to -0.7 K. As seen in Figure 2, Eymard et al's correction overcompensate after mid 2000.

Figure 7 shows the spatial distribution of the corrected TB differences over the same period of year, end of January/beginning of February, for two cycles. Cycle 30 was in 1998 and cycle 82 lately in 2003. The maps were centered to look at the spatial variability without interference from the change in mean bias with time. Note the smaller variability of the TB difference (difference in color scale) with time while we get the same spatial distribution of the difference between the two corrected TB when comparing the two maps. This can be understood by looking at Figure 1 (bottom panel). As observed for the mean 23.8 GHz brightness temperatures the difference is larger for cycle 30 than for cycle 82; that means that even when centering the maps we get more variability between the two corrections for early cycles than for latter ones since the two corrected TB converge by the end of the global ERS-2 mission. The structures are correlated with the water vapor distribution with latitude since the 23.8 GHz TB are mainly sensitive to that.

CLS -	Final Report on activities performed in 2002-2004 on the ERS2/MWR survey	Page : 72 Date : 2004-12-10
Source ref : CLS-DOS-NT-04-255	Nomenclature : -	Issue : 1 rev. 0

9.4. IMPACT ON WET TROPOSPHERIC CORRECTION

To evaluate the impact on the wet tropospheric correction, we updated all OPR 23.8 GHz TB data available with both corrections and we recomputed the wet tropospheric correction with the standard ERS-2 log-linear algorithm. Time series of the path delay mean difference is provided in Figure 8. We also compared with ECMWF estimates. This was done only over 2002-2003 because of the big change in the ECMWF model in January 2002 and in order to have consistent data from the meteorological model. Note the same behavior that was observed on the difference of corrected TB. The impact on the retrieved wet tropospheric correction is about 4 mm of change by mid 2003 while it was closed to zero in 1997. There is a slightly lower variation of the cycle averages in Scharroo et al's case. Finally the bias with ECMWF is about 0.5 mm with Scharroo et al's TB correction while it is larger at 4.0 mm with Eymard et al's correction.

Figure 9 provides the spatial distribution of path delay differences over the same cycles than for the TB, i.e. cycles 30 and 82. We observe positive biases in wet situations (Eymard et al's correction leads to wetter estimates) while we have negative biases in dry situations (Eymard et al's correction provides dryer estimates).

We compared both retrieved wet tropospheric corrections with radiosondes measurements as provided in Figure 10 (from 1 July 1996 to 31 May 2003). We observe a lower bias with radiosondes data in the case of Eymard et al's correction than in Scharroo et al's one by 1.4 mm while the standard deviations are similar.

CLS -	Final Report on activities performed in 2002-2004 on the ERS2/MWR survey	Page : 73 Date : 2004-12-10
Source ref : CLS-DOS-NT-04-255	Nomenclature : -	Issue : 1 rev. 0

9.5. CONCLUSIONS AND RECOMMENDATION

To conclude, Scharroo et al's correction took into account more OPR TB features than Eymard et al's one. They also used a longer time series to evaluate the drift and a non-linear model instead of a simple linear correction. The impact of these differences in the corrective model leads to corrected TB by Scharroo et al that are more stable over time for the period considered, cycles 005 - 085. Bias of recomputed wet tropospheric correction with ECMWF estimates is about 0.5 mm when evaluated in 2002-2003. We observed a 1.4 mm of change between the retrieved wet tropospheric corrections when comparing with the radiosondes measurements, it is larger in the case of Scharroo et al's model than with Eymard et al's one. It is acceptable. This would be reduced when applying the ENVISAT neural algorithm to recompute the wet tropospheric correction. Re-estimation of the biases and slopes between ERS-2 and ENVISAT data is necessary beforehand because they were determined with Eymard et al's TB corrective model applied.

We recommend to ERS-2 users to apply Scharroo et al's correction instead of Eymard et al's one to correct the 23.8 GHz TB for both the gain drop and subsequent instrumental drift.

9.6. REFERENCE DOCUMENTS

Scharroo R., J.L. Lillibridge, W.H.F. Smith, and E.J.O. Schrama, 2004: Cross-calibration and long-term monitoring of the microwave radiometers of ERS, TOPEX, GFO, Jason, and Envisat. *Mar. Geod.*, 27:279-297.

Eymard L., E. Obligis, and N. Tran, 2003: ERS-2/MWR drift evaluation and correction. Tech. Rep. CLS/DOS/NT/03.688, CLS, Ramonville St. Agne, France.

CLS -	Final Report on activities performed in 2002-2004 on the ERS2/MWR survey	Page : 74 Date : 2004-12-10
Source ref : CLS-DOS-NT-04-255	Nomenclature : -	Issue : 1 rev. 0

9.7. TABLES AND FIGURES

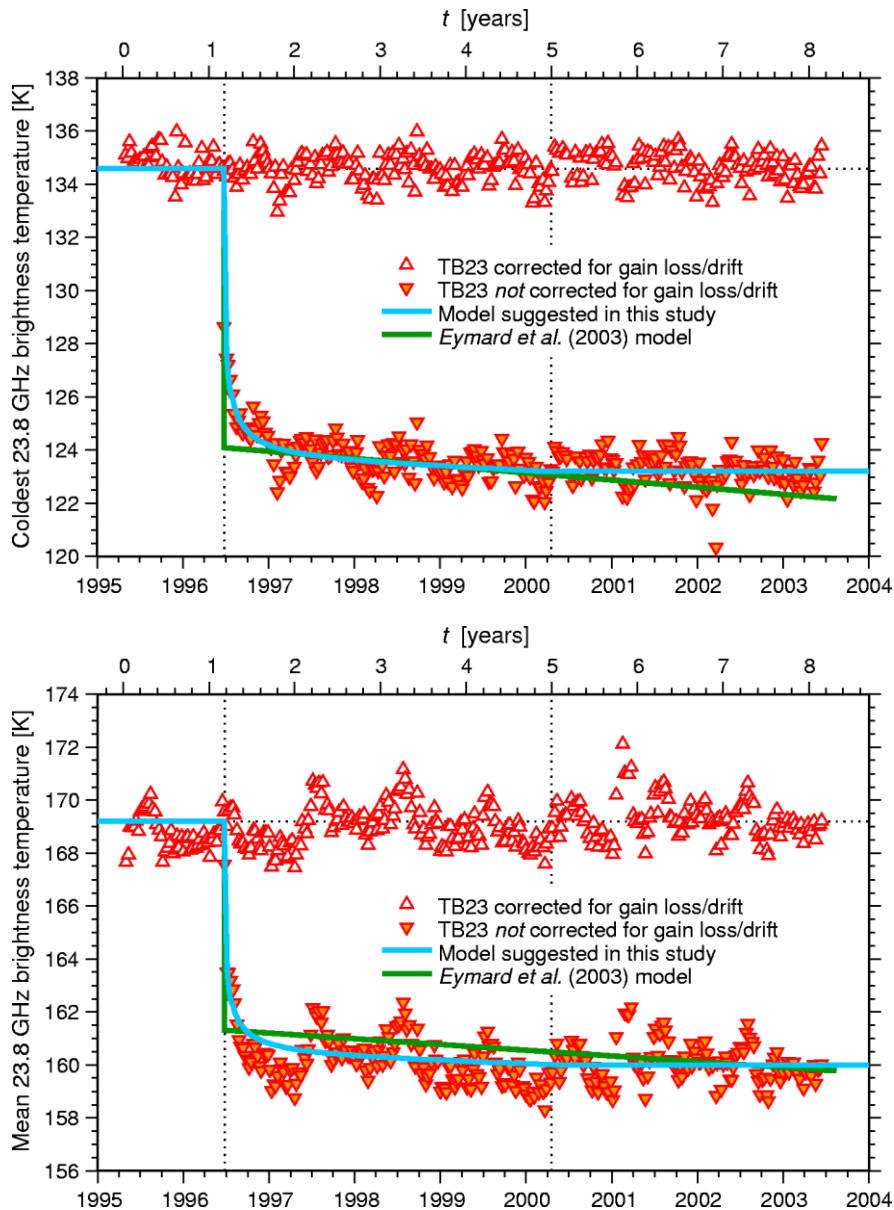


Figure 9-1 : Plots from Sharroo et al's paper (2004). ERS-2 MWR 23.8 GHz brightness temperatures (triangles), the corrective model suggested by Eymard et al (2003) (dashed), and the Sharroo et al (2004)'s model (solid). The open triangles indicate the Scharroo et al's corrected TBs. (TOP) Coldest temperatures. (BOTTOM) Mean temperatures.

CLS -	Final Report on activities performed in 2002-2004 on the ERS2/MWR survey	Page : 75 Date : 2004-12-10
Source ref : CLS-DOS-NT-04-255	Nomenclature : -	Issue : 1 rev. 0

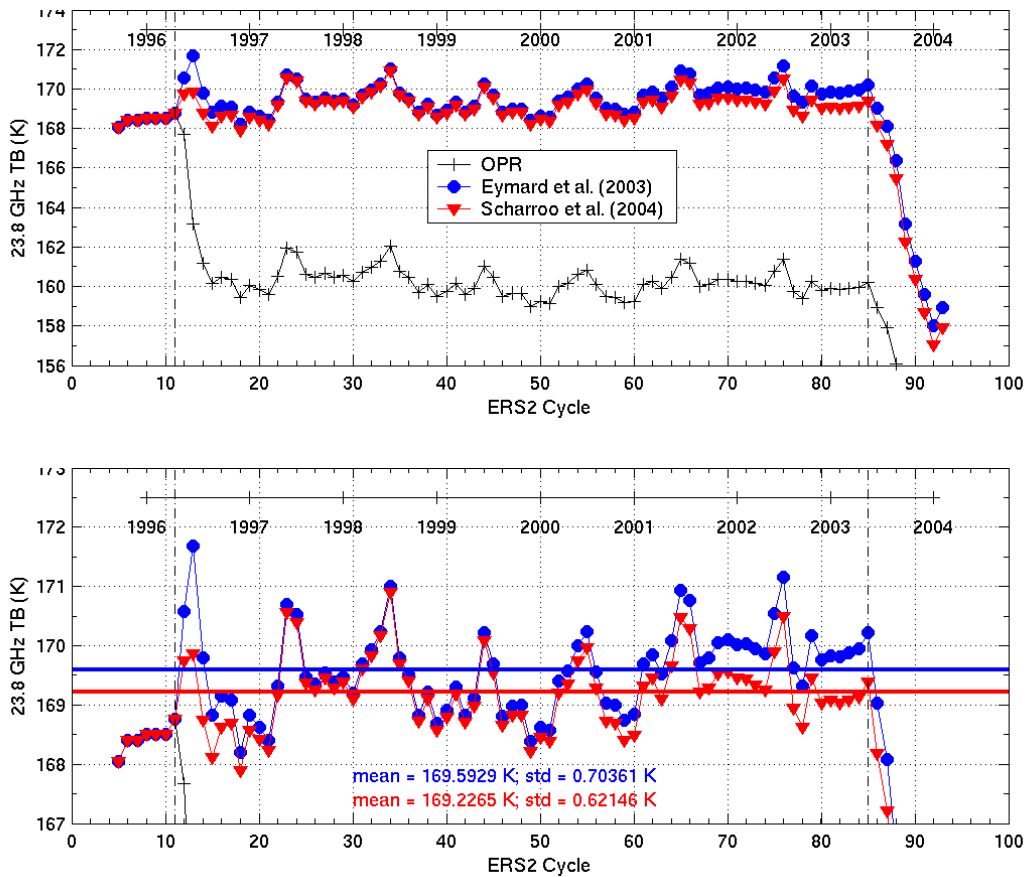


Figure 9-2 : (TOP) Time series of ERS-2 Mean 23.8 GHz TB from OPR, when corrected with Eymard et al (2003)'s model and when corrected with Scharroo et al (2004)'s model. (BOTTOM) Zoom on the corrected TB.

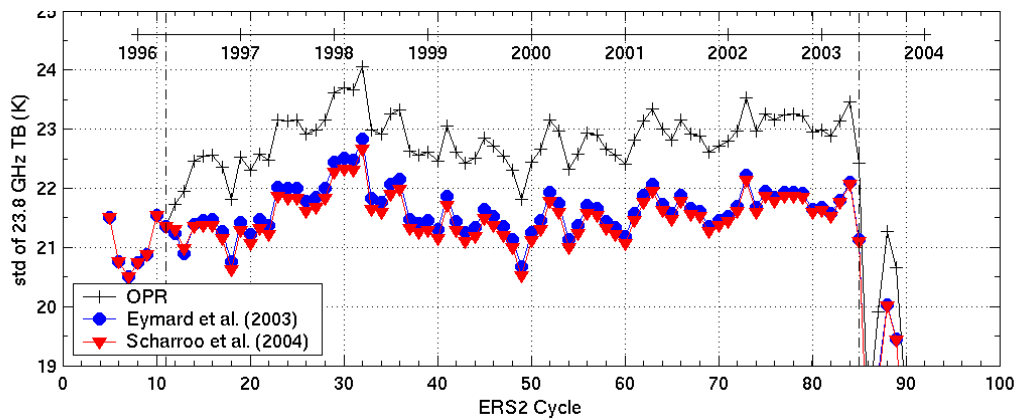


Figure 9-3 : Time series of the standard deviations of the TB computed over the cycles.

CLS -	Final Report on activities performed in 2002-2004 on the ERS2/MWR survey	Page : 76 Date : 2004-12-10
Source ref : CLS-DOS-NT-04-255	Nomenclature : -	Issue : 1 rev. 0

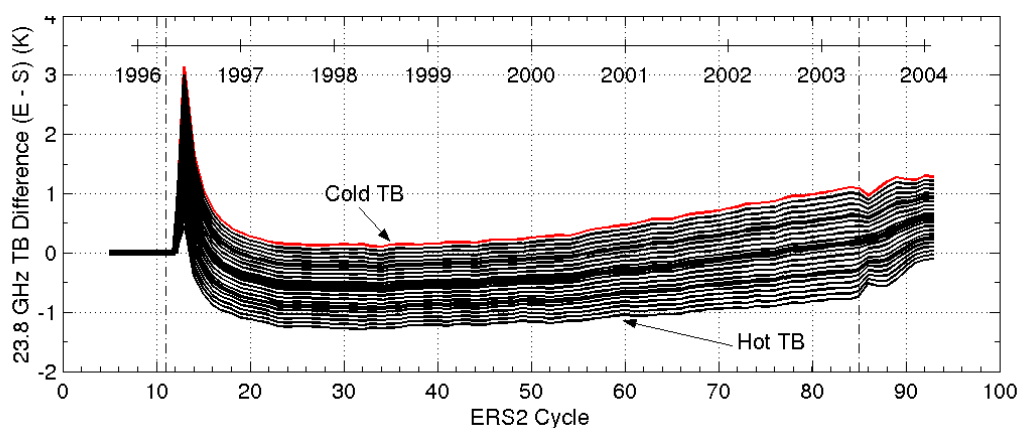


Figure 9-4 : Time series of the difference between the two corrections for different TB values.

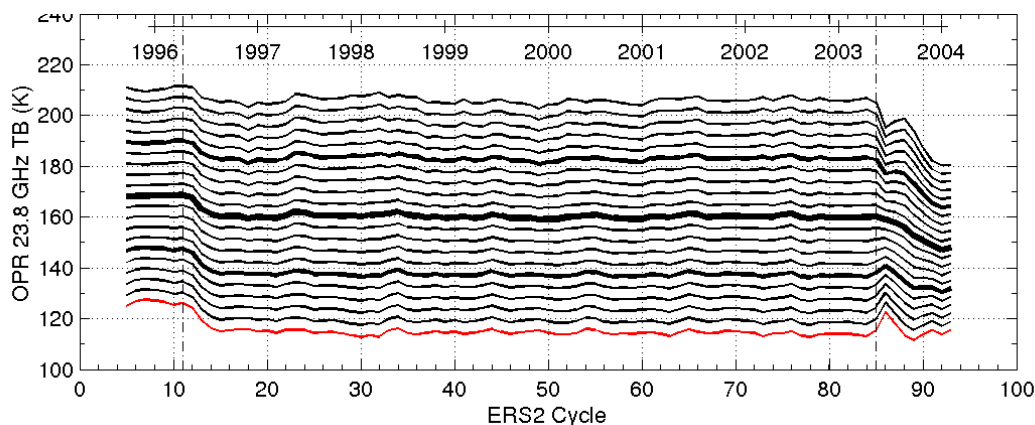


Figure 9-5 : Characterization of ERS-2 OPR 23.8 GHz TB variations in time and values. The red curve represents the (mean - 2 std) time series, the highest curve the (mean + 2 std) one. The biggest curve in the middle of the set of curves represents the cycle mean time series. We use a step of 0.2 times the std between two curves.

CLS -	Final Report on activities performed in 2002-2004 on the ERS2/MWR survey	Page : 77 Date : 2004-12-10
Source ref : CLS-DOS-NT-04-255	Nomenclature : -	Issue : 1 rev. 0

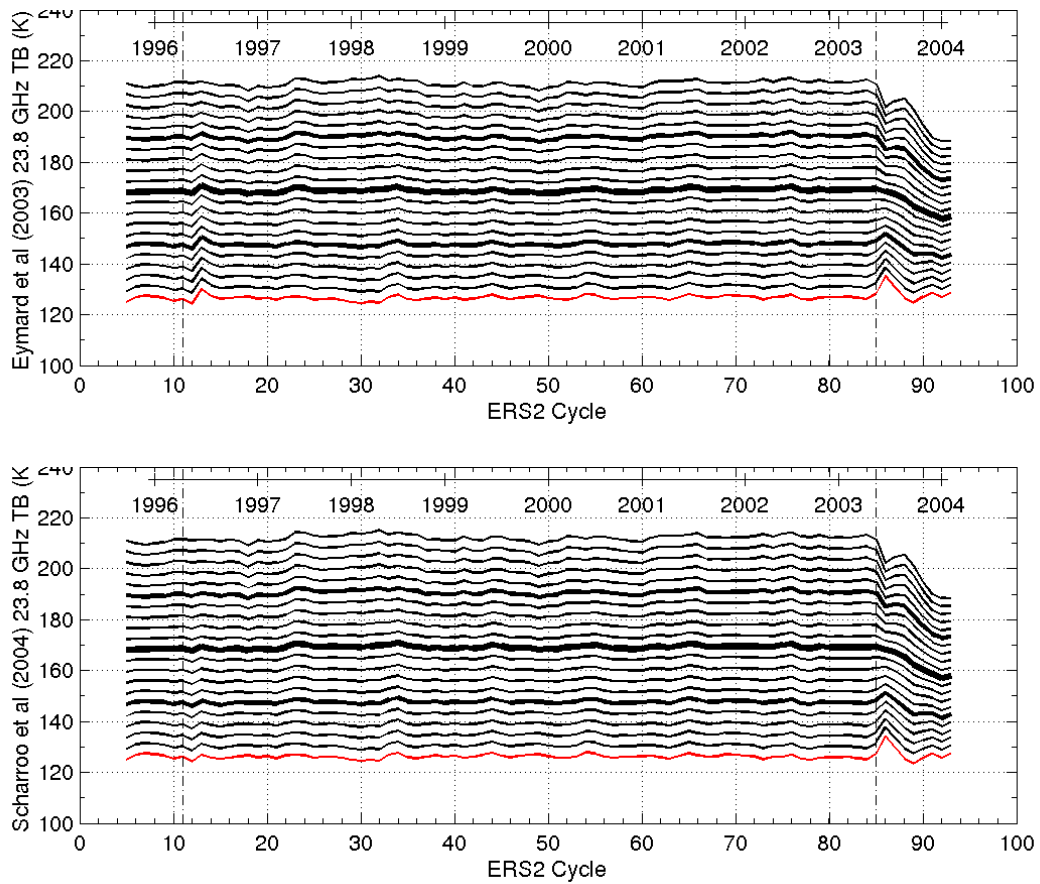


Figure 9-6 : Recomputed TB by applying the two different corrections on the TB values shown in Figure 5.

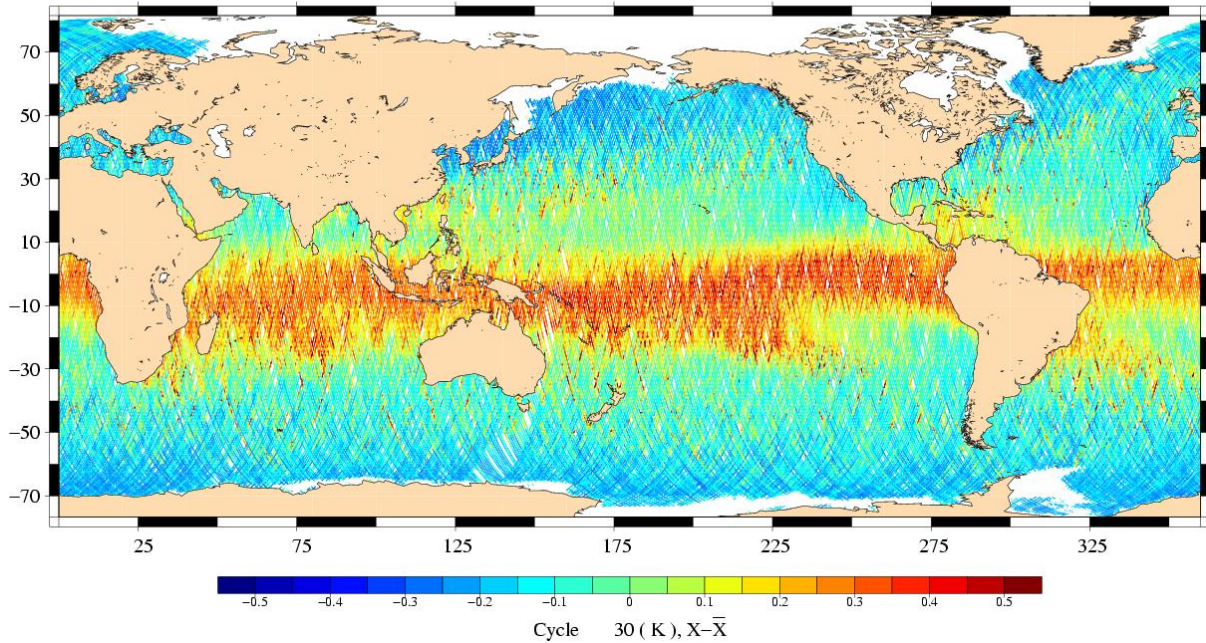
CLS -	Final Report on activities performed in 2002-2004 on the ERS2/MWR survey	Page : 78 Date : 2004-12-10
Source ref : CLS-DOS-NT-04-255	Nomenclature : -	Issue : 1 rev. 0

Table 9-1 : Statistical indicators from the linear fit on corrected TB.

	Eymard et al (2003)		Scharroo et al (2004)	
	Slope linear fit	Std(residual)	Slope linear fit	Std(residual)
mean - 2.0 std	0.0080	0.8664	0.0019	0.7550
mean - 1.8 std	0.0082	0.8164	0.0024	0.7088
mean - 1.6 std	0.0085	0.7707	0.0029	0.6677
mean - 1.4 std	0.0087	0.7302	0.0034	0.6329
mean - 1.2 std	0.0090	0.6957	0.0040	0.6054
mean - 1.0 std	0.0092	0.6682	0.0045	0.5863
mean - 0.8 std	0.0095	0.6487	0.0050	0.5763
mean - 0.6 std	0.0098	0.6377	0.0055	0.5760
mean - 0.4 std	0.0100	0.6358	0.0060	0.5853
mean - 0.2 std	0.0103	0.6430	0.0066	0.6039
mean + 0.0 std	0.0105	0.6591	0.0071	0.6308
mean + 0.2 std	0.0108	0.6834	0.0076	0.6652
mean + 0.4 std	0.0110	0.7151	0.0081	0.7058
mean + 0.6 std	0.0113	0.7532	0.0086	0.7518
mean + 0.8 std	0.0116	0.8664	0.0019	0.7550
mean + 1.0 std	0.0118	0.7969	0.0092	0.8021
mean + 1.2 std	0.0121	0.8452	0.0097	0.8560
mean + 1.4 std	0.0123	0.8974	0.0102	0.9129
mean + 1.6 std	0.0126	0.9529	0.0107	0.9723
mean + 1.8 std	0.0128	1.0111	0.0112	1.0336
mean + 2.0 std	0.0131	1.0717	0.0118	1.0967

CLS -	Final Report on activities performed in 2002-2004 on the ERS2/MWR survey	Page : 79 Date : 2004-12-10
Source ref : CLS-DOS-NT-04-255	Nomenclature : -	Issue : 1 rev. 0

cyc 30 : 23.8 GHz TB Difference (E – S) (K)



cyc 82 : 23.8 GHz TB Difference (E – S) (K)

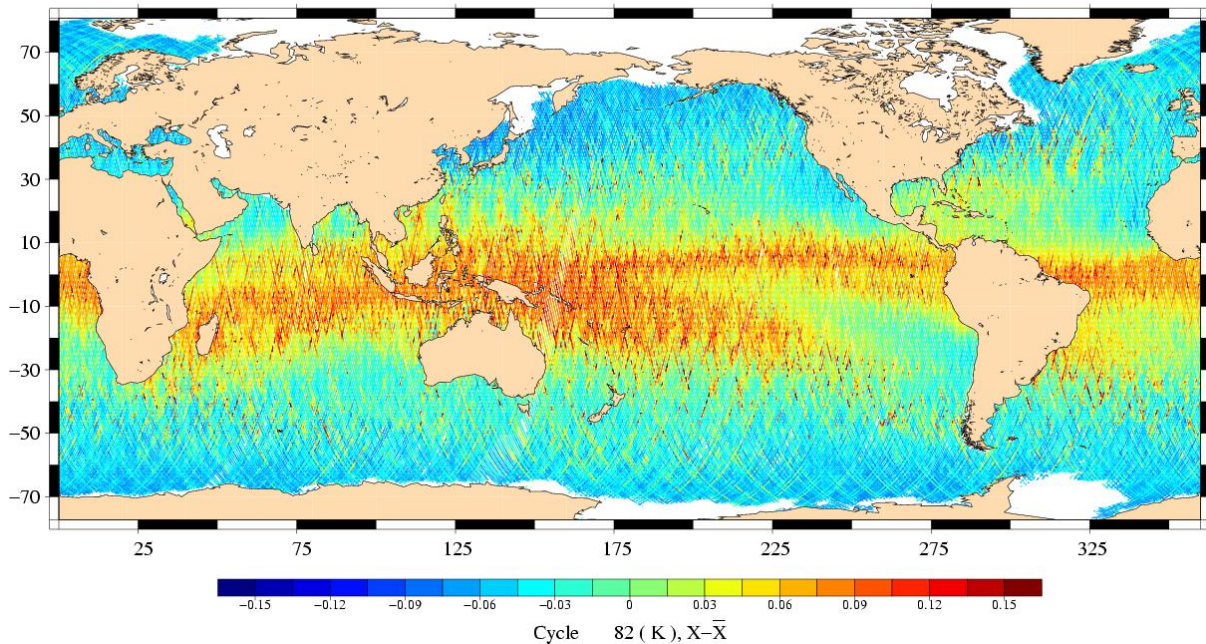


Figure 9-7: Maps of TB differences between the two proposed corrections. The maps are centered which means that the mean bias has been removed. (TOP) on cycle 30. (BOTTOM) on cycle 82.

<p>CLS</p> <p>-</p>	<p>Final Report on activities performed in 2002-2004 on the ERS2/MWR survey</p>	<p>Page : 80</p> <p>Date : 2004-12-10</p>
<p>Source ref : CLS-DOS-NT-04-255</p>	<p>Nomenclature : -</p>	<p>Issue : 1 rev. 0</p>

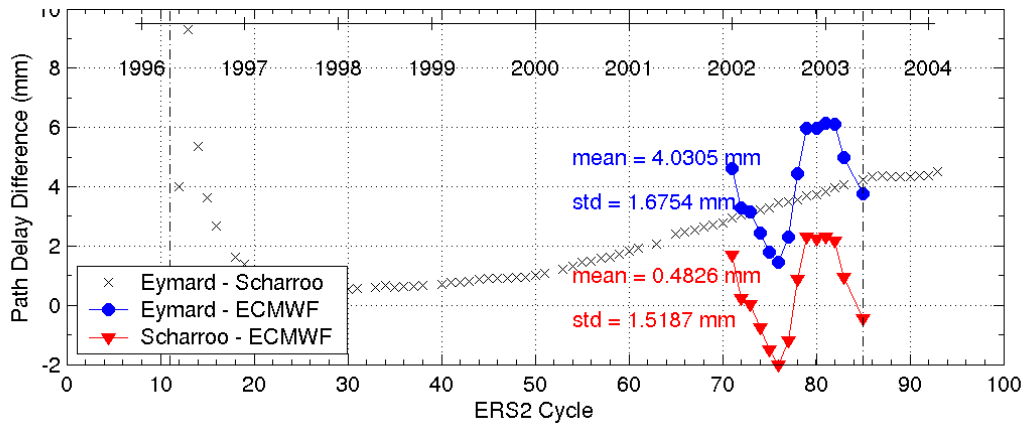
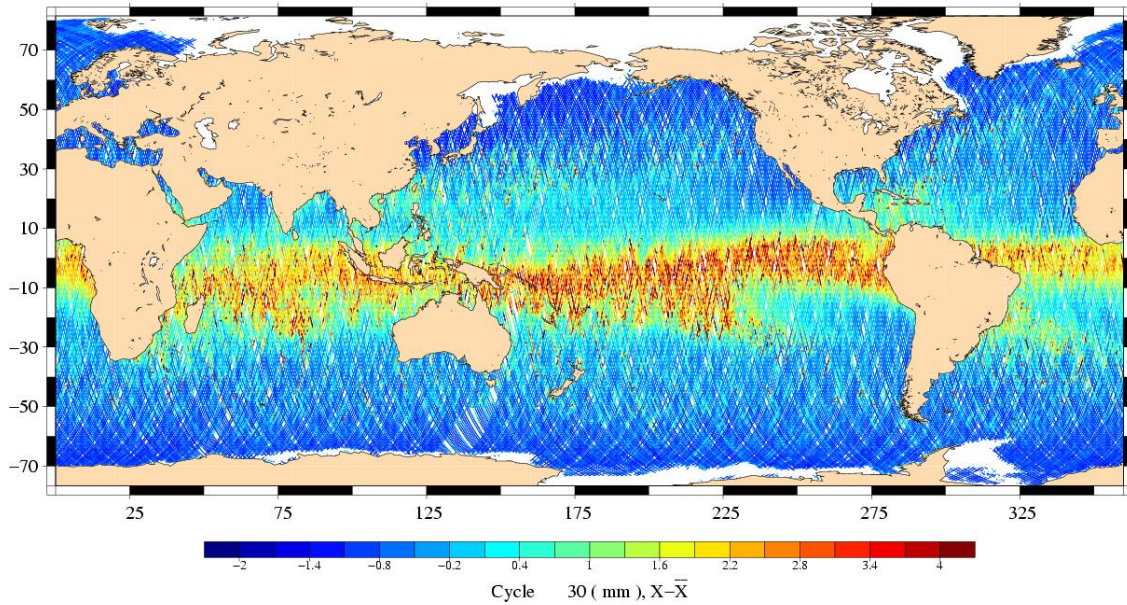


Figure 9-8: Time series of the path delay difference.

<p>CLS</p> <p>-</p>	<p>Final Report on activities performed in 2002-2004 on the ERS2/MWR survey</p>	<p>Page : 81</p> <p>Date : 2004-12-10</p>
<p>Source ref : CLS-DOS-NT-04-255</p>	<p>Nomenclature : -</p>	<p>Issue : 1 rev. 0</p>

cyc 30 : Path Delay Difference (E – S) (mm)



cyc 82 : Path Delay Difference (E – S) (mm)

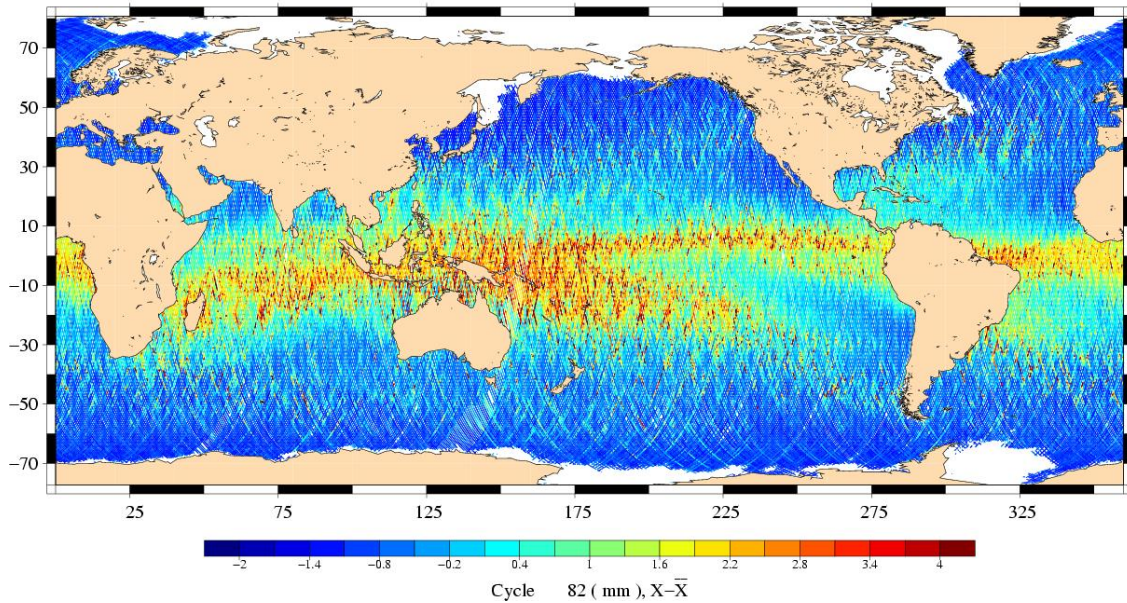


Figure 9-9 : Maps of path delay differences between the two proposed corrections. The maps are centered which means that the mean bias has been removed. (TOP) on cycle 30. (BOTTOM) on cycle 82.

CLS -	Final Report on activities performed in 2002-2004 on the ERS2/MWR survey	Page : 82 Date : 2004-12-10
Source ref : CLS-DOS-NT-04-255	Nomenclature : -	Issue : 1 rev. 0

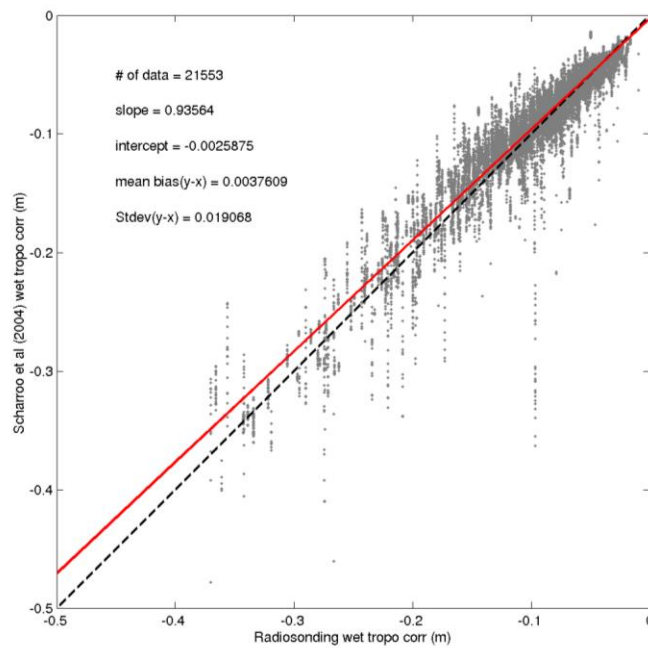
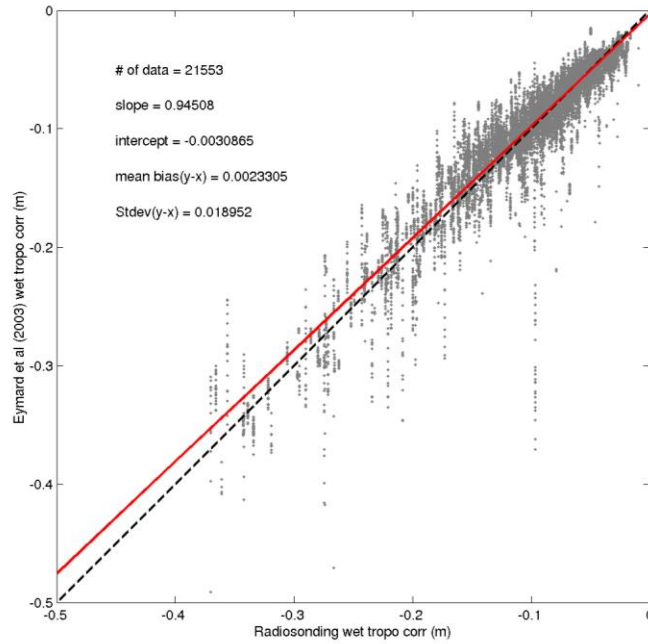


Figure 9-10: Comparison with radiosonde data. (TOP) wet tropospheric corrections recomputed from Eymard et al's corrected TB. (BOTTOM) from Scharroo et al's corrected TB.